Deliverable 2.13:

Intermediate level radioactive waste packages –

Characterization of waste and backfill degradation experiments

Work Package ACED

http://www.ejp-eurad.eu/

Document information

Project Acronym	**EURAD**
Project Title	**European Joint Programme on Radioactive Waste Management**
Project Type	**European Joint Programme (EJP)**
EC grant agreement No.	**847593**
Project starting / end date	**1st June 2019 – 30 May 2024**
Work Package No.	**WP3**
Work Package Title	**Assessment of Chemical Evolution of ILW and HLW Disposal Cells**
Work Package Acronym	**ACED**
Deliverable No.	**2.13**
Deliverable Title	**Intermediate level radioactive waste packages – Characterization of waste and backfill degradation experiments**
Lead Beneficiary	**ZAG**
Contractual Delivery Date	
Actual Delivery Date	**18 March 2024**
Type	
Dissemination level	**Public**
Authors	**Ana Mladenovic (ZAG), Yushan Gu, Leivo Markku (VTT), Erika Neeft (COVRA), Rainer Dähn (PSI)**

To be cited as:

Mladenovic, A., E. Neeft, R. Dähn, Y. Gu, and L. Markku (2022): Intermediate level radioactive waste packages – Characterization of waste and backfill degradation experiments. Final version as of 18 March 2024 of deliverable D2.13 of the HORIZON 2020 project EURAD. EC Grant agreement No.: 847593.

Disclaimer

All information in this document is provided "as is" and no guarantee or warranty is given that the information is fit for any particular purpose. The user, therefore, uses the information at its sole risk and liability. For the avoidance of all doubts, the European Commission or the individual Colleges of EURAD (and their participating members) has no liability in respect of this document, which is merely representing the authors' view.

Acknowledgement

This document is a deliverable of the European Joint Programme on Radioactive Waste Management (EURAD). EURAD has received funding from the European Union's Horizon 2020 research and innovation programme under grant agreement No 847593.

EURAD (Deliverable n° 2.13) - **Intermediate level radioactive waste packages – Characterization of waste and backfill degradation experiments**
Dissemination level: Public
Date of issue of this report: **18/03/2024**

Page 2

Status of deliverable		
	By	Date
Delivered (Lead Beneficiary)	A. Mladenovic (ZAG)	2023-08-23
Verified (WP Leader)	D. Jacques (SCK CEN)	2023-09-06
Reviewed (Reviewers)	E. Coppens (ONDRAF)	2023-11-15
Revised (Lead Beneficiary)	A. Mladenovic (ZAG)	2024-01-15
Verified (WP Leader)	D. Jacques (SCK CEN)	2024-01-17
Approved (PMO)		
Submitted to EC (Coordinator)	Andra (Coordinator)	19/03/2024

EURAD (Deliverable n° 2.13) - **Intermediate level radioactive waste packages – Characterization of waste and backfill degradation experiments**
Dissemination level: Public
Date of issue of this report: **18/03/2024**

Page 3

Executive Summary

The main objective of the ACED work package (Assessment of Chemical Evolution of ILW and HLW Disposal Cells) in the EURAD is to improve methodologies to obtain multi-scale quantitative models for the description of the chemical evolution at the disposal cell scale and to derive robust mathematical models including the most relevant processes.

For the interface and waste package scale, existing data on materials and material interfaces are combined with data from running experiments at the beginning of the project and dismantled during the project as well as few complementary new experimental set-ups for evaluating the process integration methodology. While the interface scale investigations concentrate on steel-cement and steel-clay interfaces, long-term concrete degradation and implications of waste degradation are the focus at the waste package scale.

In case of IL waste and according to existing ILW concepts in Europe, Subtask 3.1 concentrates on the analysis of long-term experiments on chemical processes, corrosion and gas generation in waste containers, the degradation of concretes in contact with lay pore water, and on the study of aggregate-cement reactions on 70–100-year-old concretes using the micro-XRF/XAS. These systems allow to study different aspects of long-term degradation of concrete and waste-concrete interaction.

This deliverable presents the results on the following experiments:

- Long-term experiments on stability of wastes - Gas Generation Experiment (Chapter 2)

This experiment is dedicated on the long-term investigation of gas generation and associated chemical changes in 200-liter carbon steel drums filled with organic waste materials under repository conditions. The experiment is in operation since 1997 and gives valuable insight into gas generation by degradation of organic waste materials and corrosion of steel materials.

- Waste package concrete/air and clay (Chapter 3)

The experiment investigates the transport of water in cement materials, the oxidation of iron sulphide minerals in blended cement in contact with saline solutions (host rock waters), and the carbonation of cement (CO_2 produced by degradation of organic waste) at different water/gas saturations.

- Investigation of concrete from the old hydroelectric power plant dams (Chapter 4)

This experiment analyses of samples from 70–100-year-old concrete from old hydroelectric power plant dams for indications of long-term aggregate reactivity. Due to their age, the samples give valuable insight into long-term aggregate reactivity, which cannot be tested with standard short term reactivity tests.

Experimental results on cementitious composites show the high importance of maintaining a high pH value, which protects these waste materials against metal corrosion, leaching and other degradation processes. Non-reactive, mineralogical stable aggregate is also a prerequisite for manufacturing of high-quality, dense concrete with low water permeability and high degradation resistance.

The experimental results provided in this report will be used in Subtask 3.3 and Task 4 for the waste package scale and disposal cell scale modelling effort, respectively. In addition, results from modelling of some of the experiments will be done in Subtask 3.3 and summarized in deliverable D2.15.

EURAD (Deliverable n° 2.13) - **Intermediate level radioactive waste packages – Characterization of waste and backfill degradation experiments**
Dissemination level: Public
Date of issue of this report: **18/03/2024**

Page 4

Table of content

EURAD (Deliverable n° 2.13) - **Intermediate level radioactive waste packages – Characterization of waste and backfill degradation experiments**
Dissemination level: Public
Date of issue of this report: **18/03/2024**

Page 5

EURAD (Deliverable n° 2.13) - **Intermediate level radioactive waste packages – Characterization of waste and backfill degradation experiments**
Dissemination level: Public
Date of issue of this report: **18/03/2024**

Page 6

List of figures

EURAD (Deliverable n° 2.13) - **Intermediate level radioactive waste packages – Characterization of waste and backfill degradation experiments**
Dissemination level: Public
Date of issue of this report: **18/03/2024**

Page 7

EURAD (Deliverable n° 2.13) - **Intermediate level radioactive waste packages – Characterization of waste and backfill degradation experiments**
Dissemination level: Public
Date of issue of this report: **18/03/2024**

Page 8

EURAD (Deliverable n° 2.13) - **Intermediate level radioactive waste packages – Characterization of waste and backfill degradation experiments**
Dissemination level: Public
Date of issue of this report: **18/03/2024**

Page 9

EURAD (Deliverable n° 2.13) - **Intermediate level radioactive waste packages – Characterization of waste and backfill degradation experiments**
Dissemination level: Public
Date of issue of this report: **18/03/2024**

Page 10

List of Tables

EURAD (Deliverable n° 2.13) - **Intermediate level radioactive waste packages – Characterization of waste and backfill degradation experiments**
Dissemination level: Public
Date of issue of this report: **18/03/2024**

Page 11

Glossary

AAR: Alkali-aggregate reaction

ACED: Assessment of Chemical Evolution of ILW and HLW Disposal Cells

ASR: Alkali-silica reaction

AFt and AFm: Calcium aluminate hydrate phases

CSH: Calcium Silicate Hydrate

CH: Calcium Hydroxide

DIC: Total dissolved carbon

EDS: Energy-dispersive X-ray spectroscopy

GGE: Gas Generation Experiment in Olkiluoto, Finland

HLW: High-level radioactive waste

ICP-OES: Inductively coupled plasma mass spectrometry

ILW: Intermediate-level radioactive waste

LLW: Low-level radioactive waste

LLW: Low-level radioactive waste

OPC: Ordinary Portland cement

PE: Polyethylene

SEM: Scanning electron microscopy

VLJ: Finnish repository for short-lived low- and intermediate level waste

XAS: X-ray absorption spectroscopy

XRF: X-ray fluorescence

EURAD (Deliverable n° 2.13) - **Intermediate level radioactive waste packages – Characterization of waste and backfill degradation experiments**
Dissemination level: Public
Date of issue of this report: **18/03/2024**

Page 12

1. Introduction

The main objective of the EURAD project ACED (Assessment of Chemical Evolution of ILW and HLW Disposal Cells) is to improve methodologies to obtain multi-scale quantitative models for the description of the chemical evolution at the disposal cell scale and to derive robust mathematical models including the most relevant processes.

The ACED approach is focusing on (i) process integration and (ii) model abstraction on three scales, interface scale, waste package scale and disposal cell scale (Figure 1-1).

1. In process integration we aim at the integration of existing scientific knowledge (and models) into models at the relevant space and time scales.
2. With model abstraction we aim at the development of methodologies to reduce model complexity in a systematic way such that an acceptable description of the chemical evolution is preserved,

For the interface and waste package scale, existing data on materials and material interfaces are combined with data from currently running experiments and few complementary new experimental set-ups for evaluating the process integration methodology. While on interface scale investigations concentrate on steel-cementitious and steel-clay interfaces, on waste package scale long-term concrete degradation and implications of waste degradation is the focus.

The upscaling between the investigated scales is defined in terms of information exchange from relatively small-scale processes (interface scale) to more complex systems at waste package scale and further to full disposal cell scale. The exchange information can take different forms such as identified critical processes, abstracted process representation, up-scaled parameter values, or simplified representation of features.

The work on waste package scale has been concentrated on the evaluation of process knowledge integration and model abstraction techniques. For the ILW waste, the focus is on cemented waste packages with metallic (iron/steel) waste and organic waste. Cement is used for waste conditioning and backfilling void space as it provides a stable encapsulant for storage and transport. In addition, the highly alkaline conditions provide a favourable environment for retarding most radionuclides, minimize other chemical reactions like corrosion of iron/steel, and reduce microbiological activity. The long-term chemical evolution of such waste packages in deep geological repositories depends to a large degree on waste package design, waste content and conditioning, and on boundary conditions imposed by the repository design and evolution.

The main aims of the performed experiments within Subtask 3.1 were to provide a high-quality input data from experiments for modelling in Subtask 3.3 and Subtask 4:

- To investigate different aspects, influential factors, evolution and reaction products of waste package degradation within the disposal cell that contains carbon steel drums filled with organic waste materials (Experiment 1: Gas Generation Experiment),
- To investigate transport rate and behaviour of water in cement materials and the oxidation of iron sulphide minerals in blended cement in contact with saline solutions (host rock waters) as well as the carbonation of cement (CO_2 produced by degradation of organic waste) at different water/gas saturation conditions (Experiment 2: Waste package concrete/air and clay experiment),
- To get insight into microstructure of historical concrete of the old hydroelectric power plant dams to recognize the stability of siliceous aggregate, the extend of degradation and type of degradation products (Experiment 3: Investigation of concrete from the old hydroelectric power plant dams),

The presented research experiments are not closely interconnected (they deal with different mechanisms/scenarios), however they have a common point in investigation of concrete resistance to

EURAD (Deliverable n° 2.13) - **Intermediate level radioactive waste packages – Characterization of waste and backfill degradation experiments**
Dissemination level: Public
Date of issue of this report: **18/03/2024**

Page 13

degradation, and, in experiment 1 and 2, the production and/or consumption of gases by waste degradation.

This report is organized as follows. After the introduction it provides information on the experiments that have been conducted in the framework of geochemical interaction between different materials in a ILW disposal cell:

1. Long-term experiments on stability of wastes – Gas Generation Experiment (Chapter 2)
2. Waste package concrete/air and clay (Chapter 3)
3. Investigation of concrete from the old hydroelectric power plant dams (Chapter 4)

In a final chapter experimental findings and eventual recommendations for modelling are summarized (Chapter 5).

EURAD (Deliverable n° 2.13) - **Intermediate level radioactive waste packages – Characterization of waste and backfill degradation experiments**
Dissemination level: Public
Date of issue of this report: **18/03/2024**

Page 14

2. Experiment 1: Gas Generation Experiment – Long-term experiments on stability of wastes

2.1 Background

Partner: VTT

Contact person: Yushan Gu

Work performed by: Markku Leivo and Yushan Gu

In Finland, intermediate and low-level radioactive waste (ILW&LLW) contains considerable amounts of cellulose and hemicellulose based material. Steel containers are used to store and dispose of the waste. The microbial degradation of cellulose and hemicellulose, together with the utilization of hydrogen generated by metal corrosion, will result in gas generation under final repository conditions. The chemical environment inside the container and steel drums will also be strongly affected. Microbially mediated ILW&LLW degradation and gas generation processes can influence the performance of multi-barrier systems, such as by accelerating corrosion and can affect the mobility of radionuclides from the repository.

A large-scale in situ Gas Generation Experiment (GGE) was established in 1997 in Olkiluoto, Finland, to simulate the gas generation and chemical changes from LLW under geological repository conditions. The experiment aims to examine the process of gas generation from cellulose-containing LLW under conditions representative of the Finnish repository, for short-lived low- and intermediate level waste (VLJ), Olkiluoto, Finland, and to improve the understanding of the involved processes, including corrosion, microbial activity, species transport, and mineralogical evolutions. The GGE has operated continually and largely uninterrupted since 1997 and has ended in the autumn of 2023. It has been regularly analysed for chemistry, gas generation, composition of gas and microbiology. Some results and analyses for the beginning 10 to 20 years are available in Small et al. (2008) and Small et al. (2017). The cumulated volume of the gas generation up until August 2021 will be presented in this report. At the very later stage of the experiment, sulfate was added in June 2020 to simulate the flow of sulfate-rich groundwater through the repository and KOH was added in August 2021 to simulate a higher pH value influenced by concrete in the repository. However, the impact of disturbances on gas generation and gas composition is out of the scope of the ACED study, so the corresponding results will not be presented in this report. Interested readers are referred to Vikman (2022).

2.2 Description

2.2.1 Experimental layup

Figure 2-1 shows the schematic layout of the large-scale GGE. The GGE comprises sixteen 200 litre carbon steel drums containing LLW from nuclear power plants at the Olkiluoto site, placed within a concrete box (mass 4000 kg), as used in the VLJ repository in Olkiluoto, that is enclosed in a 20 m^3 acid proof stainless steel gas tight reaction vessel. The LLW contained in the drums represents routine reactor operating waste and included cellulose (paper, cardboard, cotton), polyethylene, polyvinylchloride, polycarbonate, natural rubber, metal wastes, glass fibre and electrical components. The total masses of metal (including mild steel drums), cellulose and other organic polymers in the GGE at the start of the experiment were 379 kg, 620 kg and 596 kg respectively. The GGE tank was filled with 16 m^3 of locally sourced river water to provide an inoculum reflecting the plan to intentionally fill the disposal silos with water at the closure of the repository.
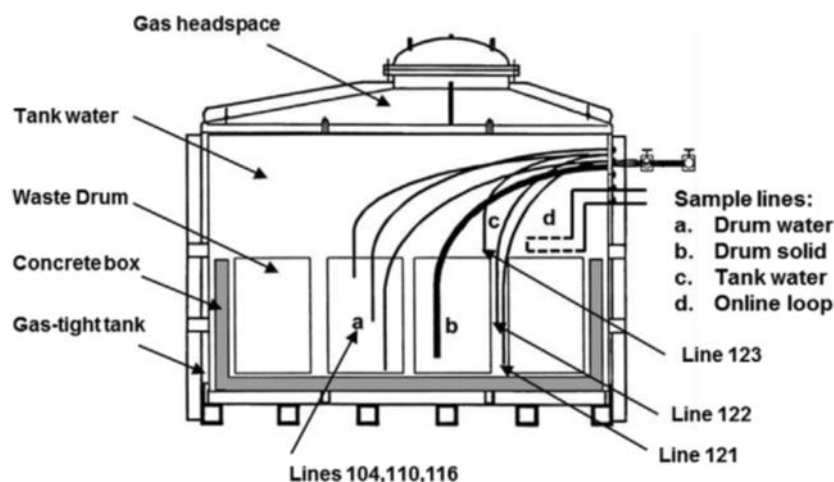
Figure 2-1: Schematic of the GGE showing different types of sampling lines (a, b, c) online analyses (d) and location of lines 104, 110, 116, 121, 122 and 123 that were used to take water samples. The dead volumes of the tubing are approximately 0.1–0.4 dm^3. Drums are normal size 200 litres steel drums (height about 0.9 m and diameter about 0.6 m). Also capsules containing a piece of drum steel and LLW were loaded to the experiment (b, drum solid) (Small et al., 2008).

2.2.2 Waste package water chemistry evolution in GGE

Some results of the experiment are presented here. Experimental results and modelling presented in detail can be seen in Small et al. (2008), Vikman et al. (2017), and Vikman (2019).

Experimental data shows that chemical conditions in various compartments of GGE tanks have been very heterogeneous. During the first years of operation of the GGE, water at the drum-lid level of the tank was alkaline (pH 10–11) but pH remained close to neutral inside the drums and in the tank water at the bottom of the tank, where there is an accumulation of organic matter originating from river water (Figure 2-2). The alkalinity of the tank water has gradually declined and stabilised at around 6.7 until June 2020, presumably as a result of CO_2 adsorbed into the tank water and microbial metabolites such as volatile fatty acids generated during the biodegradation of LLW. The surface of the concrete is likely to have been carbonated because of the high concentrations of dissolved inorganic carbon and this may have further reduced the alkaline buffering effect of the concrete.

EURAD (Deliverable n° 2.13) - **Intermediate level radioactive waste packages – Characterization of waste and backfill degradation experiments**
Dissemination level: Public
Date of issue of this report: **18/03/2024**

Page 16
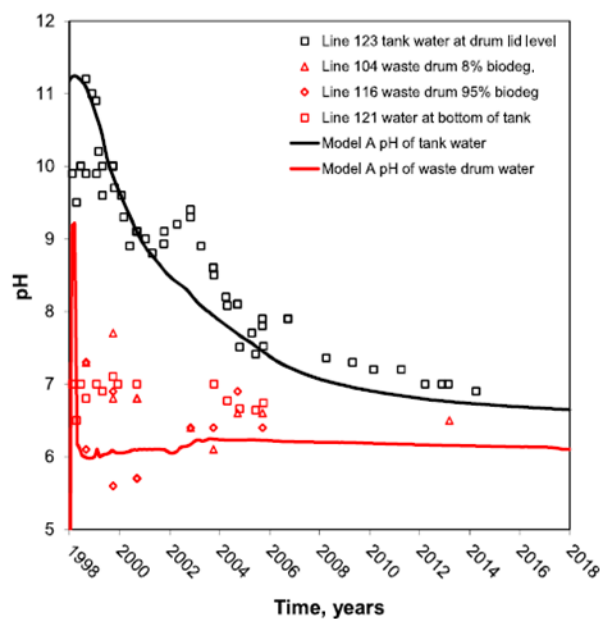
Figure 2-2: Measured pH value of water samples from sample lines from the GGE and fitted average modelled pH of model cells representing tank water and waste drum regions of the experiment (Vikman et al., 2017).

In analysing of the pH of the experiment, it is assumed that the majority of the increasing Na and K concentrations in the tank water result from diffusion from the concrete box with a smaller contribution of Na and K from the waste. The majority of the Na and K measured in tank water after 18 years therefore appear to be sourced from the alkaline pore fluid present in the concrete and this fluid has a higher proportion of K than Na (Figure 2-3), again typical for cementitious leachate.

The key parameters that affect the evolution of the tank water pH value in this model were found to be (i) the concentration of NaOH and KOH in the concrete, (ii) the diffusion coefficients of the concrete material and (iii) the rate of enzymatic cellulose hydrolysis.

EURAD (Deliverable n° 2.13) - **Intermediate level radioactive waste packages – Characterization of waste and backfill degradation experiments**
Dissemination level: Public
Date of issue of this report: **18/03/2024**

Page 17
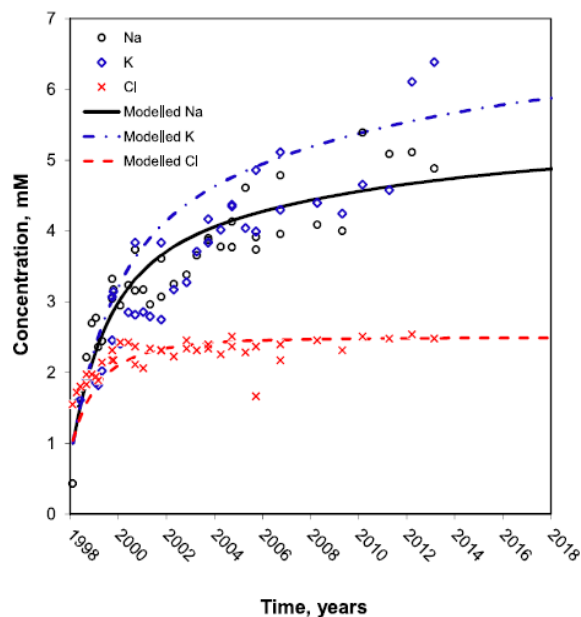
Figure 2-3: Na, K and Cl, concentration in samples of tank water (Vikman et al., 2017).

Aqueous chemistry

Figure 2-4 presents the concentration of S, C, Fe, Ca and Mg from samples of tank water from over the 18 years of operation of the GGE together with average modelled concentrations of the water filled region.

Sulphate and sulphide

Sulphate reduction is evident in the decline in sulphate concentration from around 0.5 mM during the first year of operation to below detection (2 µM) after September 2000 (Figure 2-4a). Associated with the decline in sulphate concentration significant levels of sulphide, up to 0.2 mM, were measured during 1999 and 2000. Sulphate reduction in the tank water occurs later than observed in samples from the waste drums (Small et al., 2008). Sulphate reduction appears contemporaneous with methanogenesis within the whole of the GGE, as a result of heterogeneity between the waste and water regions.

EURAD (Deliverable n° 2.13) - **Intermediate level radioactive waste packages – Characterization of waste and backfill degradation experiments**
Dissemination level: Public
Date of issue of this report: **18/03/2024**

Page 18
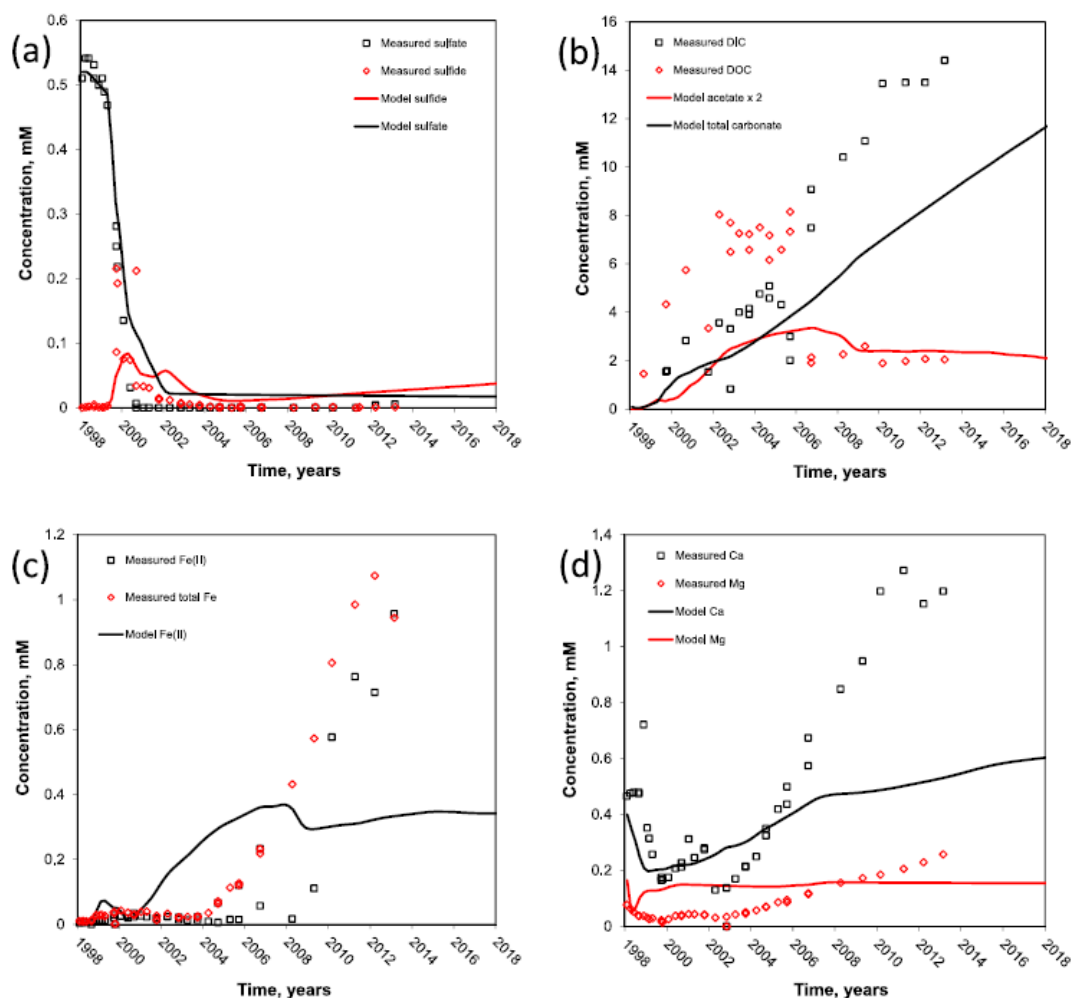
Figure 2-4: Measured concentrations of dissolved species in tank water at the drum lid level of the GGE and average modelled concentrations of tank water (a) sulphate and sulphide (b) inorganic and organic carbon (c) iron (d) calcium and magnesium (Vikman et. al, 2017)

Inorganic and organic carbon

Figure 2-4b indicates that total dissolved carbon (DIC) concentration measured in the tank water has increased during the 18 years of operation of the experiment from below 2 mM at the start of the experiment to over 14 mM in the most recent analyses. DIC concentrations recorded from the waste drums during the first 9 years of the experiment range between 6 and 25 mM (Small et al., 2008). The increasing concentration of DIC in the tank water reflects the biodegradation of cellulose materials present in the waste drums that generate CO_2 in addition to CH_4.

Iron, Calcium and Magnesium

Aqueous concentrations of Fe, Ca and Mg measured in the tank water (Figure 2-4 c and d) increased during the course of the experiment. The concentrations of these metals in tank water are lower than measured in the waste drums during the first 9 years of the experiment (Small et al., 2008). Both total Fe and Fe(2) had the highest concentrations in a drum with high cellulose compared to the drum with relatively low cellulose content, but these are still higher than the concentrations in the tank water.

The observed increase in concentration of Fe, Ca and Mg (Figure 2-4 c and d) is a consequence of the transport of species through diffusion and mixing of water from the waste drums with the tank

EURAD (Deliverable n° 2.13) - **Intermediate level radioactive waste packages – Characterization of waste and backfill degradation experiments**
Dissemination level: Public
Date of issue of this report: **18/03/2024**

Page 19

water. In addition, the significant lowering of the pH and increasing carbonate levels in the tank water during the 18 years of the experiment will affect Fe, Ca and Mg concentration through equilibria with mineral phases and sorption processes.

Gas released

The total amount of cellulose in the experiment was 620 kg originally. From gas generation it can be estimated that between 4% and 6.5% of the potentially degradable materials were disintegrated in 16 years of experiment (Vikman, 2013). This corresponded that between 1.2 kg and 5 kg is disintegrating annually. Therefore, these chemical processes will continue for a long time.

Gas generated in the test was released due to the microbiological activity. In **Erreur ! Source du renvoi introuvable.** simplified reactions for gas generation are presented.
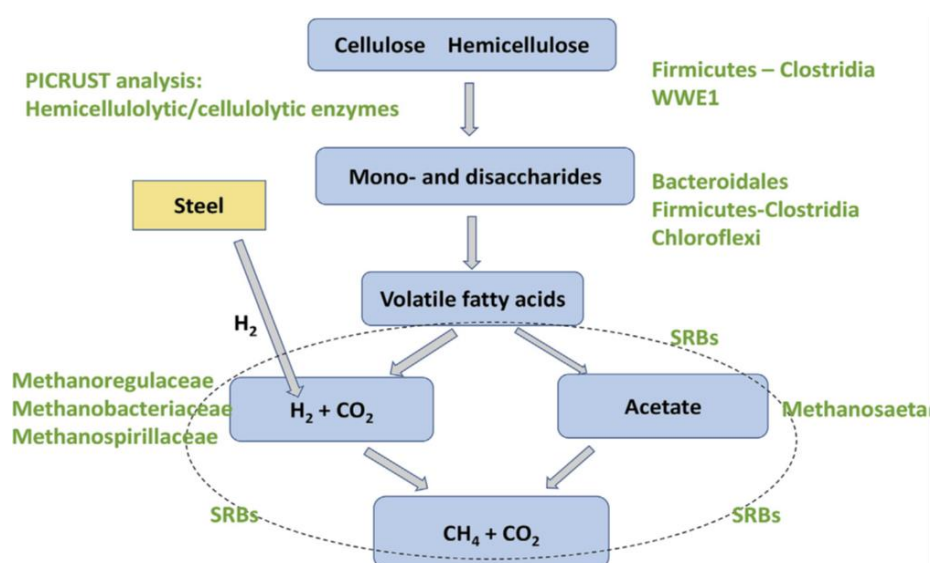
Figure 2-5: Simplified disintegration of cellulose and hemicellulose in GGE (Vikman M. M., 2019)

The measured gas amount during the test up to August 2021 was about $1 m^3$ annually, as presented in **Erreur ! Source du renvoi introuvable.** It is worth noting again that sulfate and KOH were added in June 2020 and August 2021 to investigate their impacts on gas generation, which is out of the scope of ACED. The major gasses present in the gas generated by the GGE include H_2, CH_4, CO_2, O_2, and N_2. CH_4 was detected as the first generated gas after 6 months, and it occupies a vol% between 50% and 90% in the following years. H_2 was only detected during the first 18 months of operation. O_2 concentration has been less than 0.1 vol% due to flushing out from the system. A significant amount (10-47 vol%) of N_2 was found, even though it was not analysed during the initial period. A CO_2 concentration of 3 vol% was present in the gas phase during the first two years of the operation, which is higher than the content in tank water that is in equilibrium with a pH value of 10-11. It was because the CO_2 generated in the neutral pH waste drums was not able to reach equilibrium with the alkaline tank water during the initial 4 years of the experiment, and it was released. However, CO_2 was not measured after 9 years until June 2020 when the disturbance impact of the added sulfate and KOH was studied. Theoretically, the CO_2 content should have been much higher. This "missing" CO_2 was dissolved into the water and eventually bound to concrete. The CO_2 content in the biogas is normally 30-60% (Finnish Biocycle and Biogas Association web page, 2022). On the other hand (Small et al., 2008) modelled that the CO_2 content should have been 10%. By May 2020 before the addition of sulfate, the measured gas composition includes: H_2 and O_2 with a volume fraction of less than 0.1%,

EURAD (Deliverable n° 2.13) - **Intermediate level radioactive waste packages – Characterization of waste and backfill degradation experiments**
Dissemination level: Public
Date of issue of this report: **18/03/2024**

Page 20

CH_4 with a volume fraction of 90%, and N_2 with a volume fraction of 0.38. If we assume the rest volume belongs to CO_2, CO_2 then has a volume fraction of approximately 9.42%, which is quite close to the modelled value in (Small et al., 2008).
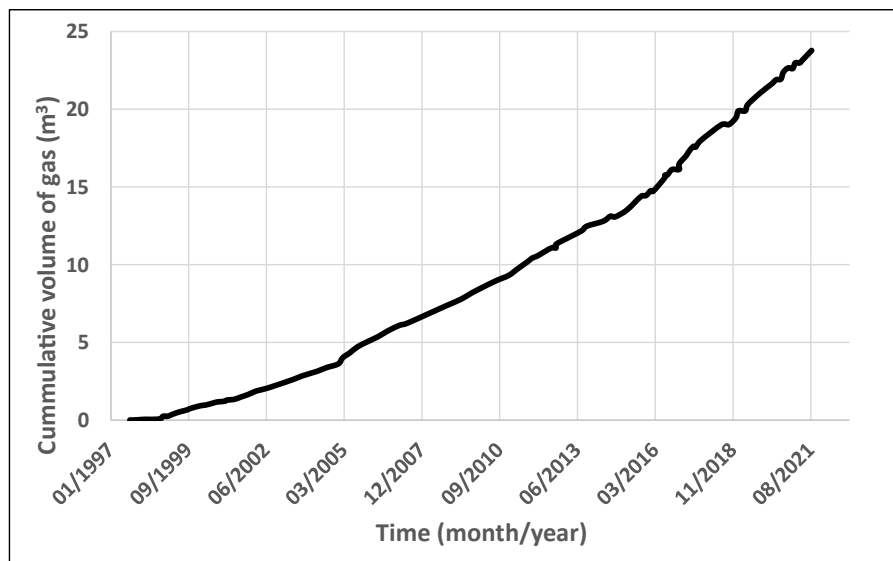
Figure 2-6: Cumulative gas generation in the GGE up to August 2021. (Note: sulfate was added in June 2020 to simulate the flow of sulfate-rich groundwater through the repository and KOH was added in August 2021 to simulate a higher pH value influenced by concrete.

EURAD (Deliverable n° 2.13) - **Intermediate level radioactive waste packages – Characterization of waste and backfill degradation experiments**
Dissemination level: Public
Date of issue of this report: **18/03/2024**

Page 21

3. Experiment 2: Waste package concrete/air and clay

3.1 Background

Partner: COVRA

Contact person: Erika Neeft

Work performed by: Erika Neeft, Alex de Best, Roos van Kleef, Ton de Bruin, Edwin Penning

Conditioned ILW contains cement that will be subject to changes when interacting with the environment. Cementitious materials, studies by COVRA in the EURAD ACED work package, are a waste package concrete and a foamed concrete/mortar. The cement content is similar (~400 kg/m^3) but the content in quartz aggregates and the size of the aggregates are different (Mladenovic et al., 2019). Figure 3-1 shows an example of the positions of the waste package concrete used to condition compacted waste in 200 litre drums. The waste package concrete has a small size in aggregates in order to eliminate as much as possible void volume in the 200 litre drum.
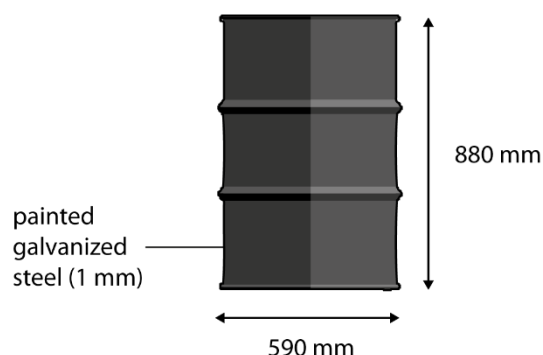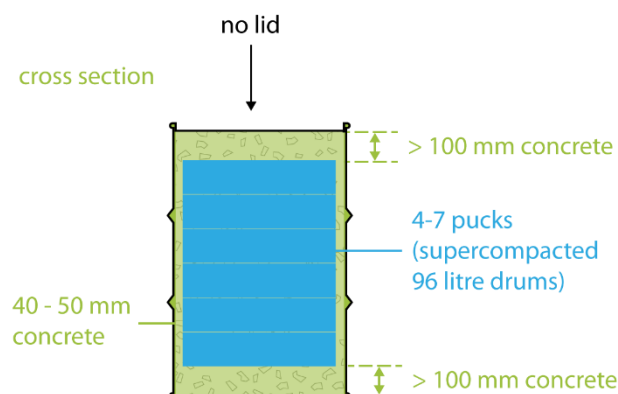
Figure 3-1: Waste package concrete (light green) used within 200 litre drums (Verhoef et al., 2016)

During storage, these 200 litre drums may be temporarily emplaced in removable concrete shells if the radiation rate is too high. The storage period is foreseen to be at least 100 years in the current Dutch policy (I&E, 2016) and these concrete shells are to be removed after sufficient decay e.g. after several decades of storage. This procedure has the aim to minimize the volume of waste for disposal. The investigated waste package concrete is also poured in permanent concrete shielding containers where this concrete surrounds 200 litre drums with cementitious conditioned radioactive (molybdenum) waste (Verhoef et al., 2016). The waste package concrete is impermeable according to NEN 12390-08 – Depth of penetration of water under pressure i.e. impermeable for engineering purposes.

EURAD (Deliverable n° 2.13) - **Intermediate level radioactive waste packages – Characterization of waste and backfill degradation experiments**
Dissemination level: Public
Date of issue of this report: **18/03/2024**

Page 22

Waste package concrete and foamed concrete are both made of blended cement containing Portland cement and blast furnace slag i.e. CEM III/B 42.5 N LH/SR. The exposure to air at different relative humidity's aims to provide sufficient quantitative data to study the ingress of gases such as carbon dioxide, but also oxygen. Ingress of oxygen can also be important in the operational phase during the implementation of geological disposal of radioactive waste for reinforced concrete or other interfaces between concrete and steel. COVRA has also exposed cubical concrete samples to synthetic clay pore water around room temperature since September 2016. Poorly indurated clay is the clay host rock investigated in the Netherlands. These clays have a porosity of around 40% (Mazurek et al., 2008). Representative results for reaction fronts within concretes during geological disposal are expected with this experiment since the diffusion values for dissolved species within the clay host rock are envisaged to be larger than the diffusion values within both types of concretes. The interpretation of these reactions can be used to predict chemical alterations on the long-term. Minor chemical effects within concrete as a result of the steel-concrete interface in the disposal concept are investigated as well, since dissolved iron is expected to be present in Dutch clay pore water.

3.2 Description

3.2.1 Fabrication of concretes

The waste package concrete for processing of waste is manufactured at the COVRA's premises. Special attention is paid to the water content of the aggregates in order to obtain a uniform processing quality of concrete. The minimum weight of batch of concrete is 300 kg and the cementitious fluid is forcedly mixed. The cementitious fluid for foamed concrete is fabricated at the COVRA laboratory in batches of several tens of kilograms with a minimum of 22 kg and maximum of 44 kg. The cementitious fluids are poured in moulds. The waste package concrete is also vibrated to remove entrapped air as much as possible. A plastic foil was added on top of each mould to prevent hydration cracks. After at least one day, hardened samples were removed from the moulds, weighted and put in a tap water bath for at least 27 days at room temperature. Some cubical samples with an edge of 5 cm have been sawn from a hardened cubical sample with an edge of 15 cm. The samples with an edge of 5 cm have a representative size since this sample size is more than 3.5 times larger than the largest size of the aggregates of 8 mm (see Table 3-3).

3.2.2 Exposure of concretes to air at relative humidity

Concrete samples have been submerged in tap water for 6 months and sawn samples have been submerged for 4.5 months. After that, these samples were exposed to different relative humidity at 20°C and 5°C. The thermal exposure at 20°C was performed by putting rows of plastic boxes next to one another in a specifically designed temperature controlled closet or in an ordinary refrigerator. The plastic boxes (Araven, 1.5 litres) are made from polypropylene. The temperature in this refrigerator was measured with a thermometer (mercury device) in order to monitor that the plastic boxes were exposed to a temperature of 5°C. The different relative humidity was made with the aim of saturated salt solutions. Cubical specimens with an edge of 5 cm were put on polyethylene (PE) cylinders in order to avoid contact between the samples and solutions. Sequentially, the weight of the samples has been measured in a laboratory at room temperature. Not always was the salt solution saturated when this measurement in weight was performed. Salt was then added again to the water in order to achieve the requested relative humidity. There was also sometimes precipitation of salt on the surfaces of a PE cylinder for the part that is not submerged in the salt solution. This precipitation progressively increases in height and can reach the samples. The cylinders were washed in those cases in order to prevent the surface of the samples being contaminated with salt. The plastic boxes were put back again either in the temperature controlled closet or refrigerator. A constant weight was

![eurad logo] European Joint Programme on Radioactive Waste Management

EURAD (Deliverable n° 2.13) - **Intermediate level radioactive waste packages – Characterization of waste and backfill degradation experiments**
Dissemination level: Public
Date of issue of this report: **18/03/2024**

Page 23

achieved after about 1000 days of exposure to a relative humidity, the minimum exposure period was 994 days and the maximum exposure period was 1004 days. There was more storage volume available for samples exposed to 20°C than 5°C. Consequently, different relative humidity has been used for 20°C than for 5°C (Neeft et al., 2021). Table 3-1 shows the different salts and other materials used to control the relative humidity of air inside the boxes.

Table 3-1: Relative humidity to which samples have been exposed

Used materials to control the air in polypropylene boxes*	Relative humidity at 5ºC	Relative humidity at 20ºC	Source
$NaOH \cdot H_2O$		6 ± 2	Wexler, 15-32
$KOH \cdot 2H_2O$	14 ± 2	10 ± 2	Wexler, 15-32
$LiCl \cdot H_2O$		11.31 ± 0.31	IUPAC, 15-33
$MgCl_2 \cdot 6H_2O$	33.60 ± 0.28	33.07 ± 0.18	IUPAC, 15-33
K_2CO_3	43.2 ± 0.5	43.1 ± 0.3	ASTM, 15-33
$Mg(NO_3)_2 \cdot 6H_2O$	58.86 ± 0.43	54.38 ± 0.23	IUPAC, 15-33
$NaCl$	75.65 ± 0.27	75.47 ± 0.14	IUPAC, 15-33
KCl	87.67 ± 0.45	85.11 ± 0.29	IUPAC, 15-33
K_2SO_4	98.5 ± 0.9	97.6 ± 0.9	ASTM, 15-33
Wet cotton	≈100 (99.9)	≈100 (99.9)	COVRA
Submerged in demineralized water	> 100	> 100	

*Pages 15-32 and 15-33 from Handbook of Chemistry and Physics 96th Edition, 2015-2016.

In the previous century, a working area for the radiation protection unit in COVRA's waste processing facility consisted of a wall made from concrete cubes with an edge of 15 cm. A number of these cubes had been manufactured in October 1993 to check the quality of the concrete waste packages. In 2018, during the refurbishment of this protection unit, a number of these concrete cubes became superfluous. One cube was saved for further analysis and put in a separate plastic box without a lid in larger plastic box in July 2018. That larger plastic box was earlier filled with synthetic clay pore solution that was aimed to be kept at a temperature of 20°C. The heating of the synthetic clay pore solution caused some evaporation of the water. The lid of the larger plastic box minimized the water leaving the plastic box but also caused droplets falling into the plastic box in which the cube manufactured in 1993 was emplaced. This cube was destructed in April 2022.

3.2.3 Exposure of concretes to clay solution

Concrete samples have been put on a grid in two large plastic boxes. More than 200 litres of synthetic clay pore water is present in a plastic box (Mladenovic et al., 2019) with inside dimensions 910 mm×1110 mm×610 mm. A lid (C305) was put on each plastic box and regularly lifted in order to check e.g. the temperature of the water. The water was aimed to be kept around 20°C with small heating devices. After the initially installed electrical heating device with thermostat (Macben, 230 V monophase) broke down, two aquarium heaters (Fluval, E300, 375 litres) were installed in each plastic box. The precision of the installed temperature is 0.5°C according to the description. Long-term practice of concrete cubes in tap water at COVRA however makes that the installed temperature should be a few degrees higher than the requested temperature. Later on, the aquarium heaters in the plastic box with samples of waste package concrete and certified foamed concrete malfunctioned, probably due to a too low water level arising from some evaporation of water. Another plastic box with foamed concrete made with CEM I functioned until April 2022. From April 2022, all non-destructed samples are kept in the specifically designed temperature controlled closet in plastic boxes on top of PE cylinders but still submerged in the saline solution. The temperature within the storage facility in

EURAD (Deliverable n° 2.13) - **Intermediate level radioactive waste packages – Characterization of waste and backfill degradation experiments**
Dissemination level: Public
Date of issue of this report: **18/03/2024**

Page 24

which the plastic box was emplaced is also monitored. The minimum in temperature was 7.1°C and the maximum temperature was 22.8°C, the average temperature was 15.2°C.

3.3 Material involved: Chemical composition

3.3.1 Cement

Commercially available cements are used for the manufacturing of the concrete samples. Table 3-2 shows that the chemical compositions between different suppliers are similar. The types of cements were:

- Portland cement (Betonpocket, 2019): CEM I 52.5 N – SR3/NA from Heidelberg cement;
- Most currently by COVRA used blast furnace slag cement which is a blend of 20-34% Portland cement and 66-80% blast furnace slag: CEM III/B 42.5 N-LH/SR from ENCI;
- Historically by COVRA used blast furnace slag cement that was a blend of 35-64% Portland cement and 35-65% blast furnace slag: CEM III/A probably from ENCI.

Table 3-2: Average oxide compositions of different used types of cement in wt.%

Cement type	CaO	SiO$_2$	Al$_2$O$_3$	MgO	Fe$_2$O$_3$	SO$_3$	Na$_2$O	K$_2$O	Source
CEM I 52.5 N SR3 LA	63.5	21.3	3.5	2.0	4.3	2.6	0.10	0.63	CCM, 2016
CEM I 52.5 R_SR3 LA	66.4	22.1	3.7	0.7	4.2	2.6	0.24	0.38	Holcim, 2013 Na$_2$O equiv. 0.49
CEM III/A 42.5 N	48	28	9.6	4.9	2.0	2.3	0.16	0.91	HCM,2020
CEM III/B 42.5 N LH/SR LA	48	29	9.9	6.0	1.3	2.4	0.29	0.61	HCM,2020
CEM III/B 42.5 N LH/SR*	45	28	11	-	1	2.88	Na$_2$O-equiv. 0.59		ENCI,2016

SR Sulphate resistance to prevent delayed ettringite formation, SR3 contains less than 3 wt.% of tricalcium aluminate,

LH Low hydration heat cement,

LA Low alkali cement to prevent alkali silica reaction indicated in the Belgian standard but not always in the Dutch standard.

3.3.2 Concrete recipes

Table 3-3 and Table 3-4 show the recipes to manufacture waste package concrete and foamed concrete. The exact recipe used to manufacture the waste package concrete fabricated on 13 July 2016 has been electronically registered. The waste package concrete fabricated on 6 October 1993 is not yet available in electronic form only on paper. It would take some time to find the exact recipe for 6 October 1993. Waste package concrete is however fabricated in batches and the recipes hardly differ between the different batches. The recipe published in a report (Roovers, 1994) has been included in Table 3-3 since this recipe is most similar to the recipe used for the waste package concrete fabricated on 6 October 1993. The recipes for the foamed concretes are digitally registered and also published (Mladenovic et al., 2019; Neeft et al., 2021).

Table 3-3: Recipes for waste package concretes

Component	Mix casted 13 July 2016	kg m^{-3}	mix casted 6 October 1993	kg m^{-3}
Cement	CEM III/B 42.5 N LH/SR	402	CEM III/A	≈ 410
Dutch tap water		184		≈ 176
Superplasticiser	TM OFT-II B84/39 CON. 35% (BT-SPL)	5	OFT-2 84/39 Tillmann	≈ 3
Fine aggregate	Quartz sand: 0-4 mm	827	Sand: 0-2 mm	≈ 858
Coarse aggregate	Quartz gravel: 2-8 mm	866	Gravel: 2-8 mm	≈ 930

EURAD (Deliverable n° 2.13) - **Intermediate level radioactive waste packages – Characterization of waste and backfill degradation experiments**
Dissemination level: Public
Date of issue of this report: **18/03/2024**

Page 25

Table 3-4: Recipes for foamed concretes

Component	Type casted 6, 8 and 9 September 2016	kg m^{-3}	Type casted 17 May 2016	kg m^{-3}
Cement	CEM III/B 42.5 N LH/SR	411	CEM I 52.5 N - SR3/NA [b]	417
Dutch tap water		144		165
Superplasticiser	TM OFT-II B84/39 CON. 35% (BT-SPL)	4		
Foaming agent	TM 80/23	5	TM 80/23	< 1
Fine aggregate	Quartz sand : 0-2 mm	1131	Quartz sand : 0-2 mm	1018

3.3.3 Synthetic Dutch poorly indurated clay pore water

Table 3-5 shows the applied recipe to make clay pore water with a composition that is considered to be representative for the clay pore water in Dutch poorly indurated clay with the present available knowledge. Sand has been added in sufficient amounts to prevent undersaturation of the silicon concentration. Some oxidation of iron occurred, this oxidation resulted from colourless water into orange water (Mladenovic et al., 2019).

Table 3-5: Recipe for the synthetic clay pore solution

Solids	Gram for 1 litre Dutch clay pore water
NaCl	24.475
$MgCl_2$	5.137
Na_2SO_4	4.107
$CaCl_2$	1.177
KCl	0.712
$NaHCO_3$	0.656
KBr	0.102
H_3BO_3	0.043
NaF	0.003846316
KI	0.0010
$FeCl_3$	0.011139946
$AlCl_3$	0.000346111

3.4 Solid or interface characterisation

All solid characterisations are performed from fractured surfaces. All cubical specimens with an edge of 5 cm and foamed concrete with an edge of 10 cm could be split with a chisel by hand. The aim was to chisel the specimen in the middle but it was not always succeeded to split the specimens in two equal blocks. Figure 3-2 shows some examples. The cubical specimen of waste package concrete with an edge of 15 cm needed to be fractured with a compression testing machine since the required load needed to split the specimen could not be provided by hand.

EURAD (Deliverable n° 2.13) - **Intermediate level radioactive waste packages – Characterization of waste and backfill degradation experiments**
Dissemination level: Public
Date of issue of this report: **18/03/2024**

Page 26
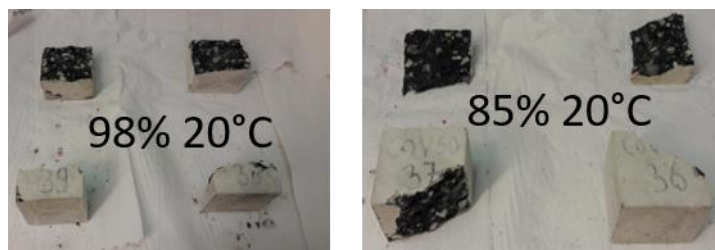
Figure 3-2: Examples of chiselled specimens with an edge of 5 cm, waste package concrete exposed to a relative humidity of 98% at 20°C (left) and 85% at 20°C (right)

3.4.1 Carbonation profiles

3.4.1.1 Method

According to NEN-EN 14630 (Products and systems for the protection and repair of concrete structures – Test methods – Determination of carbonation depth in hardened concrete by the phenolphthalein method), only chiselled concrete to reveal an adequate area of freshly broken concrete is appropriate to determine the carbonation profile. A photograph was taken of the freshly broken concrete surface. The surface was sprayed with a phenolphthalein solution. The solution contains 1 gram phenolphthalein indicator in ethyl alcohol (70 ml) diluted in demineralised water (100 ml). The aim was to take a photograph within 30 seconds of the sprayed surface. This aim was often achieved but a photograph was always obtained within 60 seconds. The photograph should allow sufficient time to measure the carbonation depth.

3.4.1.2 Impact of preparation of surface

If indicated, cut surfaces are used e.g. (Papadakis et al., 1991) but these surfaces can give misleading results because these surfaces can expose and reactivate non hydrated cement particles in otherwise fully carbonated concrete according to NEN-EN 14630. In Papadakis et al. (1991), however, complete hydration was assumed by putting the specimens in $Ca(OH)_2$ saturated solutions at 30°C for 90 days.

3.4.1.3 Impact of time

If indicated, the time taken after spraying to determine the carbonation depth can also be 24 hours e.g. (Papadakis et al., 1991). The result will not be accurate enough if the colour changes slowly and/or the boundary is diffuse which may indicate partial carbonation zones according to NEN-EN 14630. Papadakis et al. (1991) refer however to RILEM (1984) specification Measurement of hardened concrete carbonation depth. There is also a difference in time between NEN standards. In NEN-EN 13295 – Products and systems for the protection and repair of concrete structures – Test methods – determination of resistance to carbonation, the requested time after spraying the phenolphthalein solution is 60±5 minutes while it is 30 seconds in NEN-EN 14630.

3.4.1.4 Photographs from exposure to air and water

Most cubical specimens exposed to air have been made with blended cement with blast furnace slag. The fractured surfaces of concrete with this blended cement are dark blue if no oxidation occurred. This feature makes it hard to identify a rim of carbonation if the concrete is not oxidised. The specimen exposed to air for several decades in Figure 3-3 seems to have at first glance a smaller oxidation front

EURAD (Deliverable n° 2.13) - **Intermediate level radioactive waste packages – Characterization of waste and backfill degradation experiments**
Dissemination level: Public
Date of issue of this report: **18/03/2024**

Page 27

than carbonation front but it is hard to see. Modelling of the results may elucidate if it is possible to have a larger carbonation front than oxidation front.
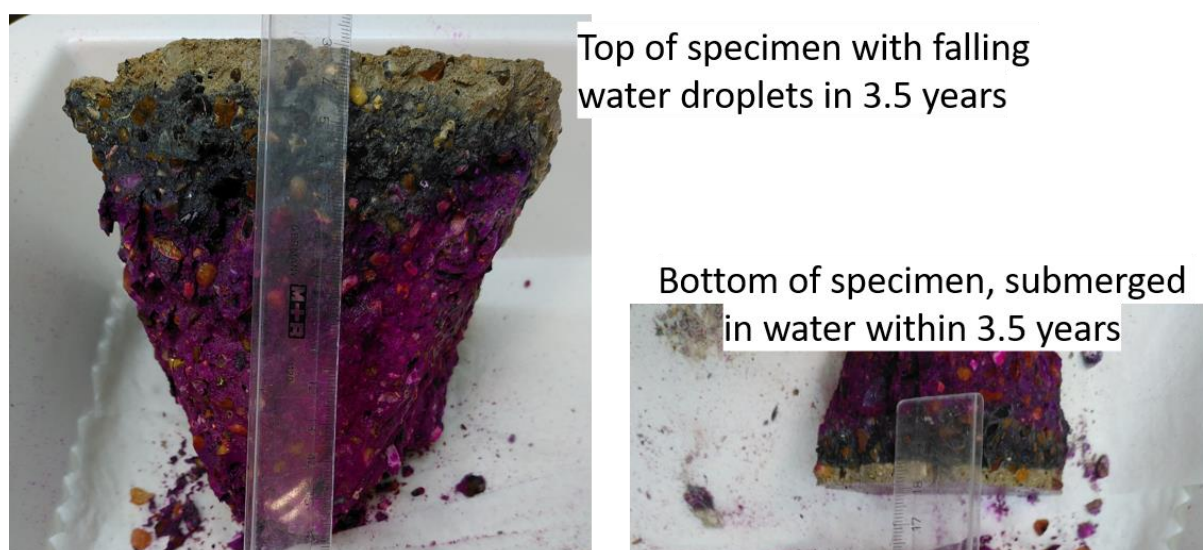
Figure 3-3: Carbonation rim of waste package concrete (1993, CEM III/A) with an edge of 15 cm after exposure to air for several decades. Bottom of specimen became submerged by water in a period of 3.5 years as explained in section 3.2.2.

All 'lab-controlled' specimens (in Figure 3-4, to Figure 3-7) seem to show larger oxidation fronts than carbonation fronts after exposure to air for about 1000 days which makes it easy to identify carbonation fronts, especially at low relative humidity's.

Some 'lab-controlled' specimens of waste package concrete with an edge of 5 cm are oxidised especially at low relative humidity's. These specimens clearly show one very small rim e.g. 0.6 mm to 1.2 mm at a relative humidity of 33% at 20°C or no rims for waste package concrete, especially if specimens have been fabricated from sawing a cubical specimen with an edge of 15 cm. The single rim for waste package concrete is therefore assumed to be highly related to the hardening stage in the mould when the surface is only separated from air by a thin foil since any reaction front should start at the corners of a specimen. However, the single rim at a relative humidity of 98% at 20°C is clearly not carbonated but this single rim is carbonated at 75% at 20°C which makes the origin entirely to the hardening not convincing. Carbonation rims are hardly visible after exposure for about 1000 days at relative humidity's lower than 98% (perhaps 85%) at 20°C for waste package concrete. At 5°C, it is not clear whether relative humidity's equal to or lower than a relative humidity 59% are necessary to achieve a carbonation rim since many sawn pieces have been used at this temperature which reduces the possibility to have a single rim due to the hardening stage.

Only some 'lab-controlled' specimens of foamed concrete show carbonation rims that continue at another edge of the specimen e.g. 2.1 mm to 2.2 mm at a relative humidity of 10% at 20°C. These rims can more clearly be attributed to carbonation for a period of about 1000 days. Carbonation rims are visible after exposure for about 1000 days at relative humidity's equal to or lower than 75% (perhaps at 85%) at 20°C for foamed concrete. At 5°C, it is clear that relative humidity's equal to or lower than 59% are necessary to achieve a carbonation rim but carbonation as a function of the relative humidity cannot be observed.

EURAD (Deliverable n° 2.13) - **Intermediate level radioactive waste packages – Characterization of waste and backfill degradation experiments**
Dissemination level: Public
Date of issue of this report: **18/03/2024**

Page 28
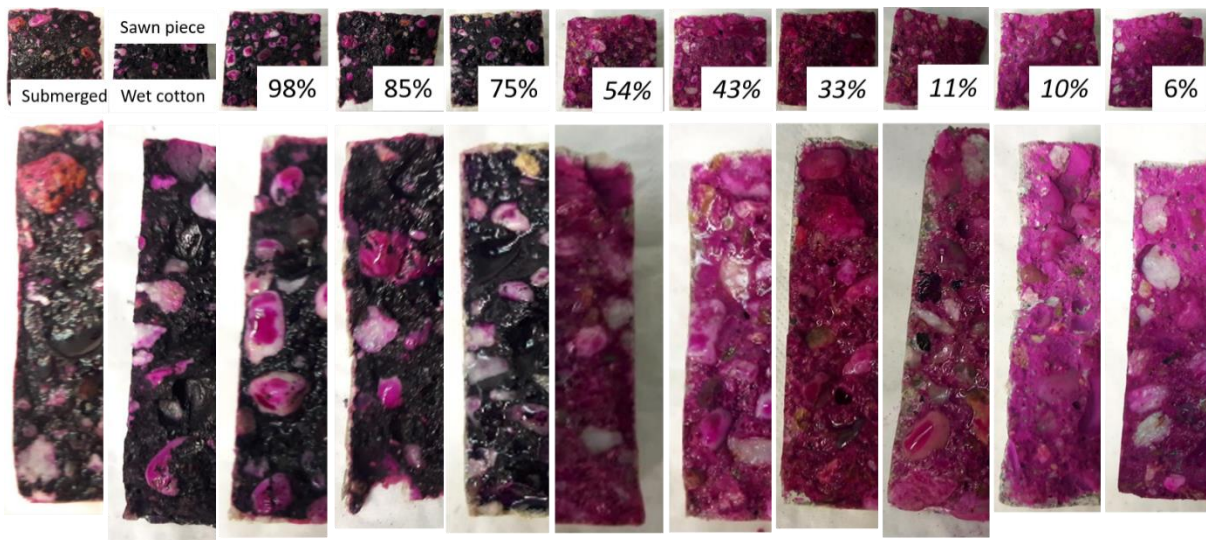
Figure 3-4: Carbonation rims at 20°C for waste package concrete after about 1000 days exposure to a relative humidity of cubical samples with an edge of 5 cm (sometimes exposure to a higher relative humidity)
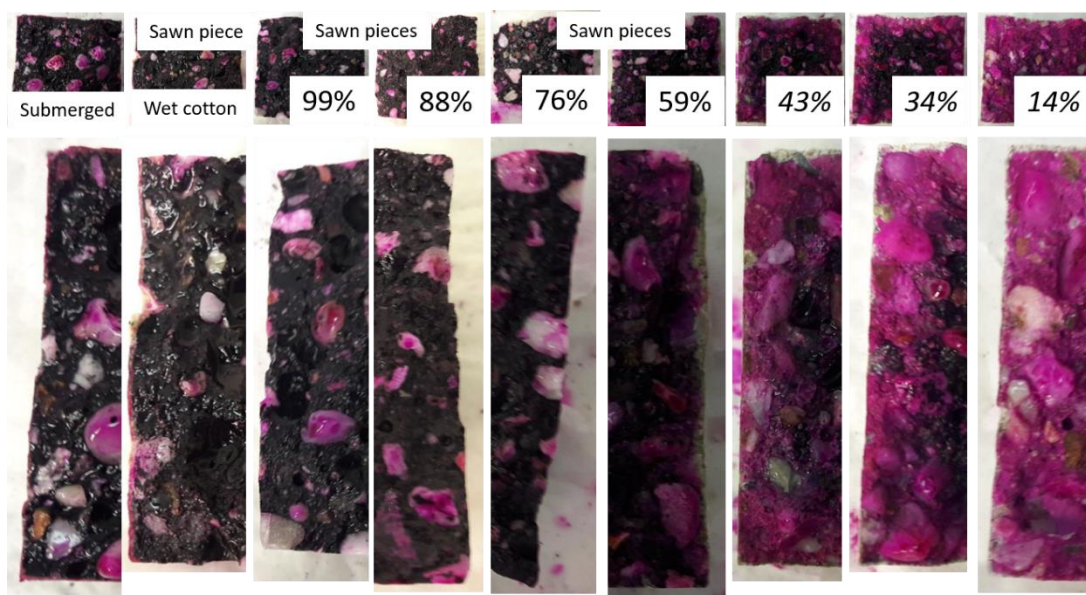
Figure 3-5: Carbonation rims at 5°C for waste package concrete after about 1000 days exposure to a relative humidity of cubical samples with an edge of 5 cm (sometimes exposure to a higher relative humidity, sawn piece means that specimen has been sawn from cubical specimen with an edge of 15 cm before exposure)

EURAD (Deliverable n° 2.13) - **Intermediate level radioactive waste packages – Characterization of waste and backfill degradation experiments**
Dissemination level: Public
Date of issue of this report: **18/03/2024**

Page 29
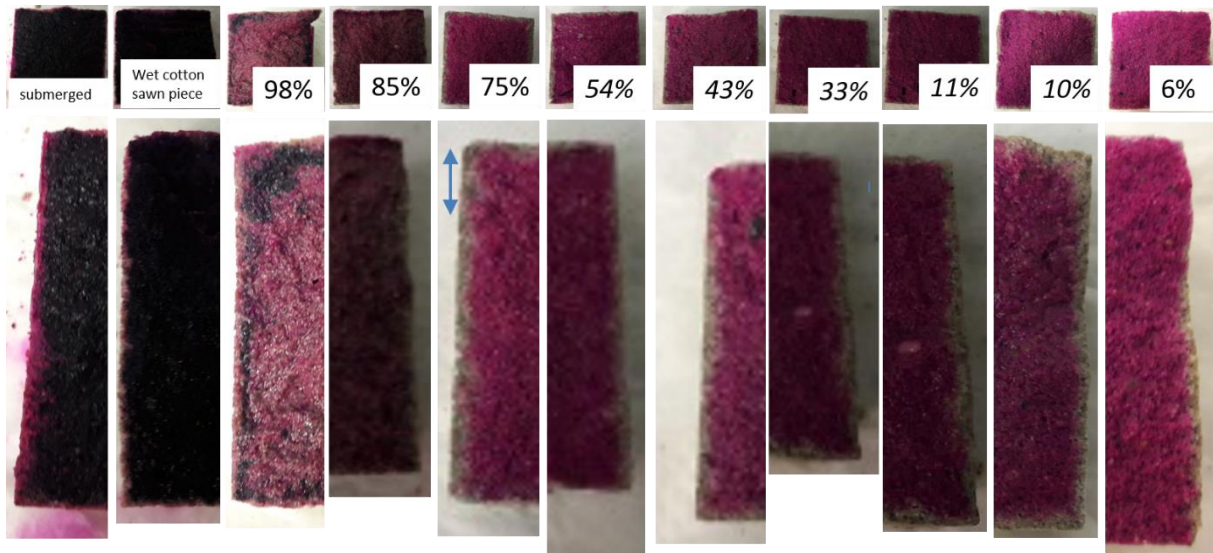
Figure 3-6: Carbonation rims at 20°C for foamed concrete after 1000 days exposure to a relative humidity of cubical samples with an edge of 5 cm (sometimes exposure to a higher relative humidity, sawn piece means that specimen has been sawn from cubical specimen with an edge of 15 cm before exposure)
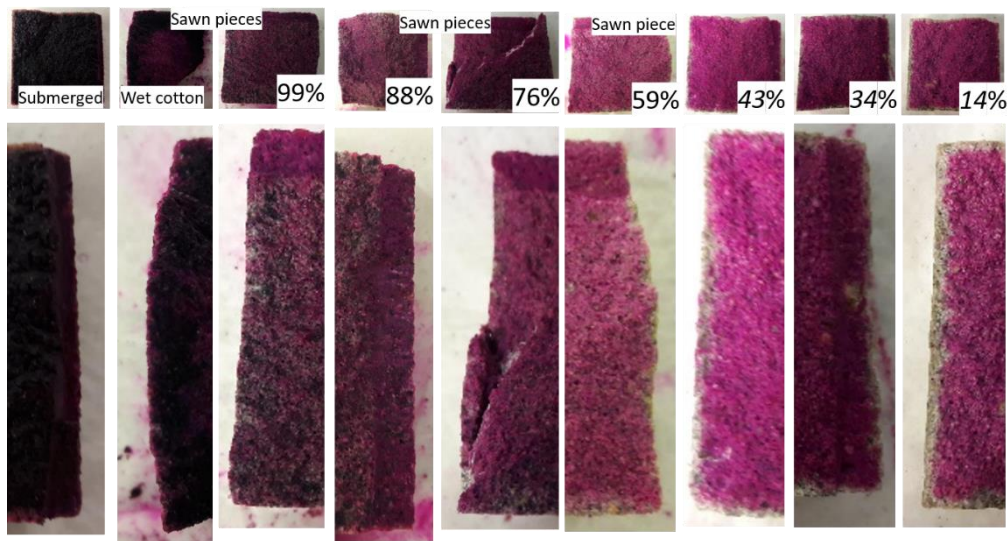
Figure 3-7: Carbonation rims at 5°C for foamed concrete after 1000 days exposure to a relative humidity of cubical samples with an edge of 5 cm (sometimes exposure to a higher relative humidity, sawn piece means that specimen has been sawn from cubical specimen with an edge of 15 cm before exposure)

3.4.1.5   Photographs from exposure to saline solution

Foamed concrete made with CEM I also has quite a dark colour which makes it difficult to observe carbonation rims (Fig. 3-8). The oxidised rims for foamed concrete made with CEM III/B also seems to be carbonated with a rim of about 1.0 to 1.5 mm.

EURAD (Deliverable n° 2.13) - **Intermediate level radioactive waste packages – Characterization of waste and backfill degradation experiments**
Dissemination level: Public
Date of issue of this report: **18/03/2024**

Page 30
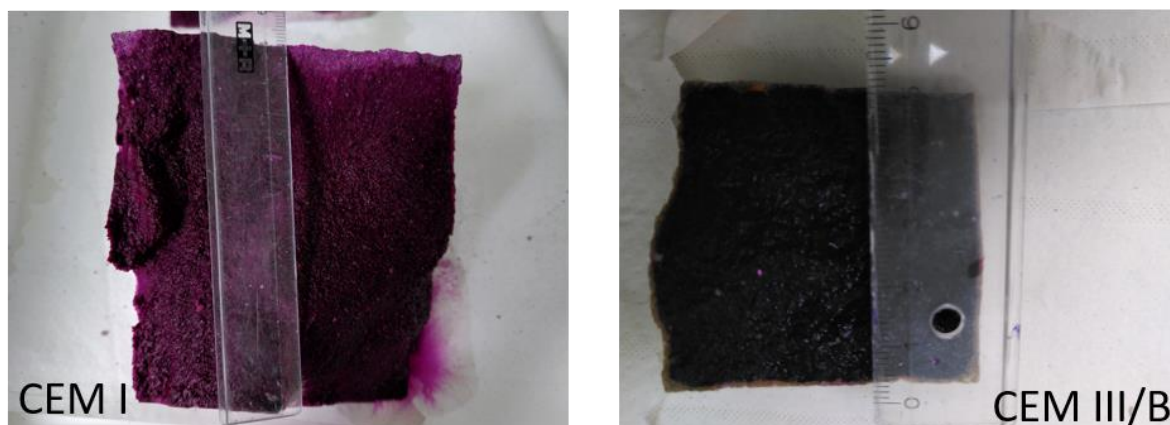
Figure 3-8: Carbonation rims around 20°C for foamed concrete made with CEM I (edge 10 cm) and CEM III/B (edge 5 cm) after to the saline solution in Table 3-5 for 5$\frac{1}{2}$ years

3.4.2 Oxygen profiles

3.4.2.1   Method

Concrete made with cement blended with blast furnace slag contains initially pyrite (or another iron-sulphide mineral) in trace amounts. The oxidation of pyrite into an iron-sulphate mineral turns the colour of concrete from dark blue into grey. These oxygen reaction fronts are determined by the access to oxygen. A photograph was taken of the freshly broken concrete surface i.e. before the spraying with the phenolphthalein solution.

3.4.2.2   Photographs from exposure to air and water

Figure 3-9 shows clearly larger oxygen fronts at the top of the sample of about 1 cm compared to the bottom of the samples of about 0.6 cm for the waste package concrete manufactured in 1993.
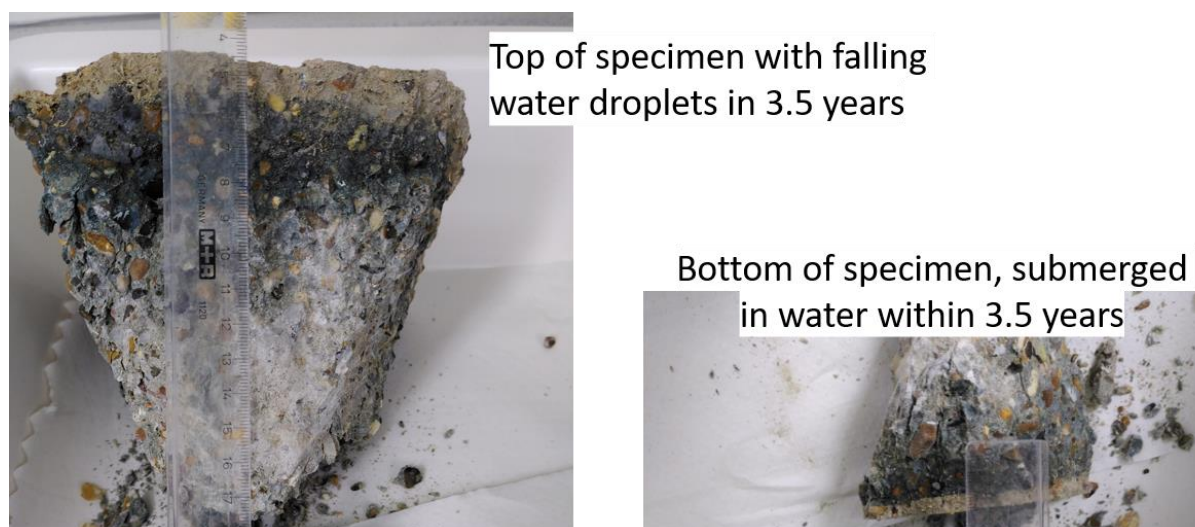
Figure 3-9: Oxygen reaction front of waste package concrete (1993, CEM III/A) with an edge of 15 cm after exposure to air in the waste processing facility for several decades. Bottom of specimen became submerged by water in a period of 3.5 years as explained in section 3.2.2.

EURAD (Deliverable n° 2.13) - **Intermediate level radioactive waste packages – Characterization of waste and backfill degradation experiments**
Dissemination level: Public
Date of issue of this report: **18/03/2024**

Page 31

For the 'lab-controlled' specimens, the waste package concrete (Figure 3-10 and Figure 3-11) as well as the foamed concrete (Figure 3-12 and Figure 3-13) clearly show an increasing oxygen reaction front with decreasing relative humidity to which the specimens have been exposed. The effect of temperature is also clear. For waste package concrete, areas with limited oxidation are still visible for specimens exposed to a relative humidity of 34% at 5°C while these areas are absent for specimens exposed to a relative humidity of 54% and lower at 20°C. The effect of porosity is also clear. Foamed concrete has no clear oxygen fronts at relative humidity's at 98% or 99%. Only submerged specimens still have non-oxidised areas. Some 'lab-controlled' specimens of waste package concrete clearly show one very small oxidation rim or no rims for waste package concrete, especially if specimens have been fabricated from sawing a cubical specimen with an edge of 15 cm. Single rim for waste package concrete is therefore highly related to the hardening stage in the mould when the surface is exposed to air since any reaction front should start at the corners of a specimen.
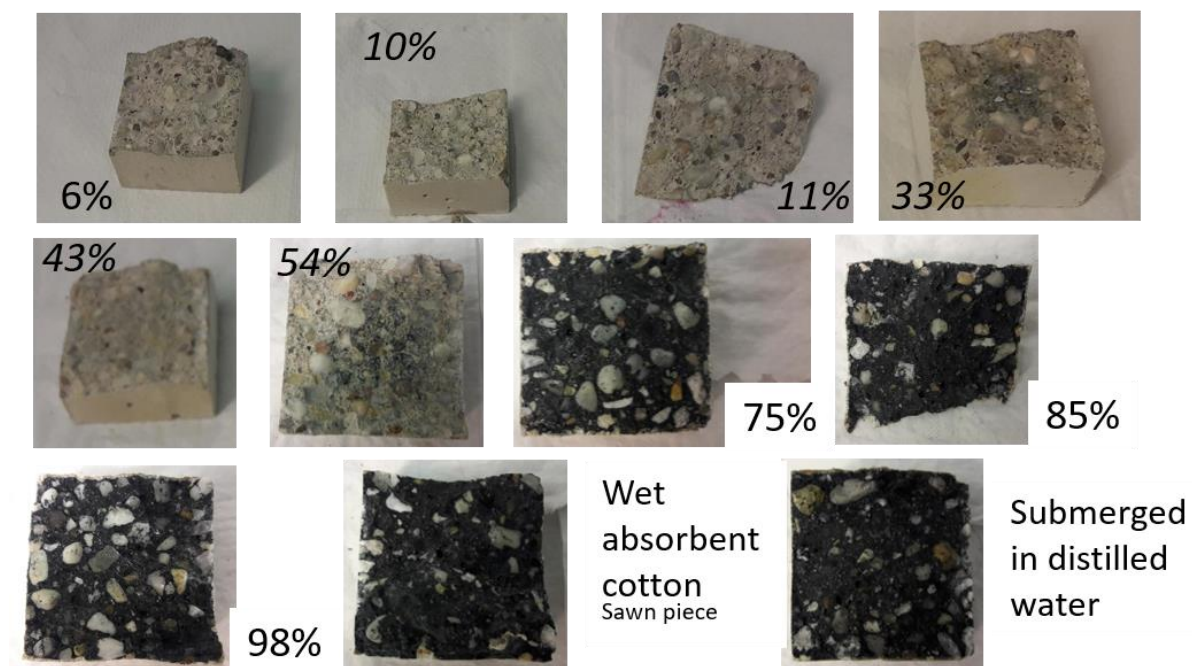
Figure 3-10: Oxidation at 20°C for waste package concrete after 1000 days exposure to a relative humidity of cubical samples with an edge of 5 cm (sometimes exposure to a higher relative humidity)

EURAD (Deliverable n° 2.13) - **Intermediate level radioactive waste packages – Characterization of waste and backfill degradation experiments**
Dissemination level: Public
Date of issue of this report: **18/03/2024**

Page 32
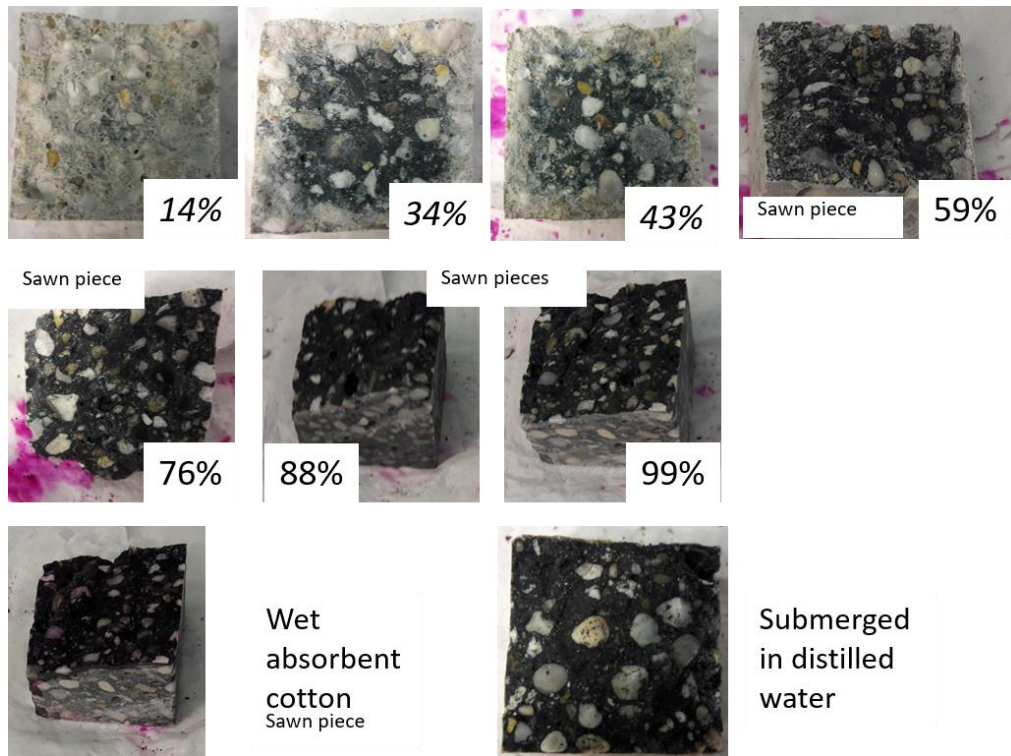
Figure 3-11: Oxidation at 5°C for waste package concrete after 1000 days exposure to a relative humidity of cubical samples with an edge of 5 cm (sometimes exposure to a higher relative humidity, sawn piece means that specimen has been sawn from cubical specimen with an edge of 15 cm before exposure)

Figure 3-12: Oxidation at 20°C for foamed concrete after 1000 days exposure to a relative humidity of cubical samples with an edge of 5 cm

EURAD (Deliverable n° 2.13) - **Intermediate level radioactive waste packages – Characterization of waste and backfill degradation experiments**
Dissemination level: Public
Date of issue of this report: **18/03/2024**

Page 33
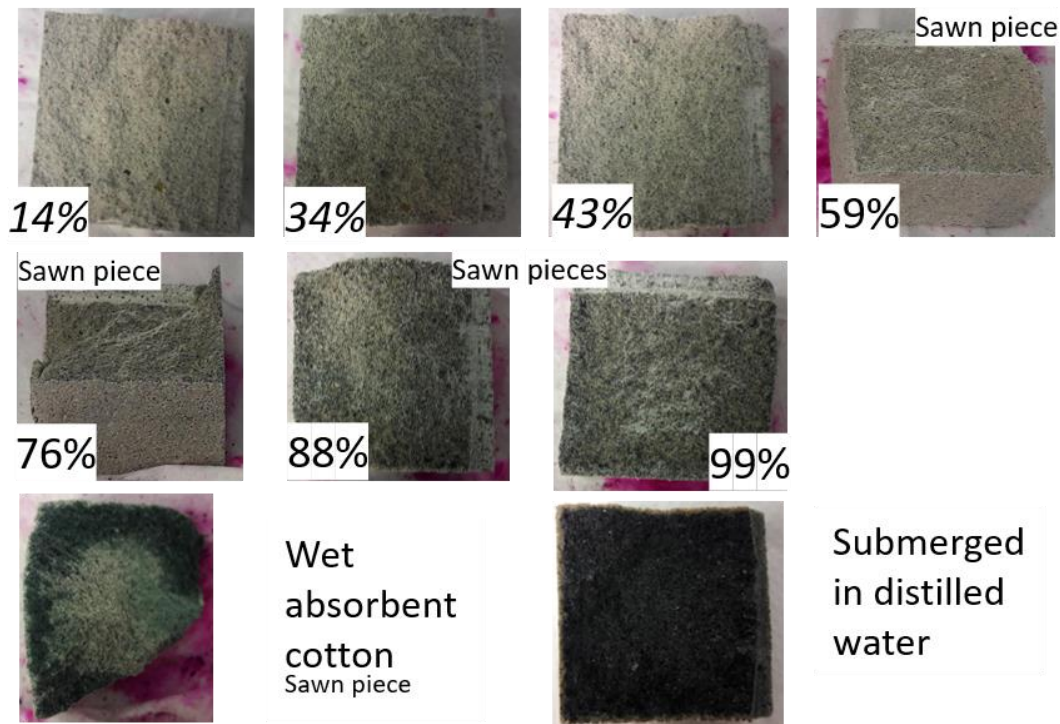
Figure 3-13: Oxidation at 5°C for foamed concrete after 1000 days exposure to a relative humidity of cubical samples with an edge of 5 cm (sometimes exposure to a higher relative humidity, sawn piece means that specimen has been sawn from cubical specimen with an edge of 15 cm before exposure).

3.4.2.3   Photographs from exposure to saline solution

Figure 3-14 shows that oxidation rims cannot be observed for waste package concrete (sawn specimens). For foamed concrete, these oxidation rims start at the corners of the specimen after $4^{1}/_{3}$ years of exposure to a saline solution and can be observed at every edge after $5^{1}/_{2}$ years of exposure.

EURAD (Deliverable n° 2.13) - **Intermediate level radioactive waste packages – Characterization of waste and backfill degradation experiments**
Dissemination level: Public
Date of issue of this report: **18/03/2024**

Page 34

$4^1/_3$ years

$5^1/_2$ years
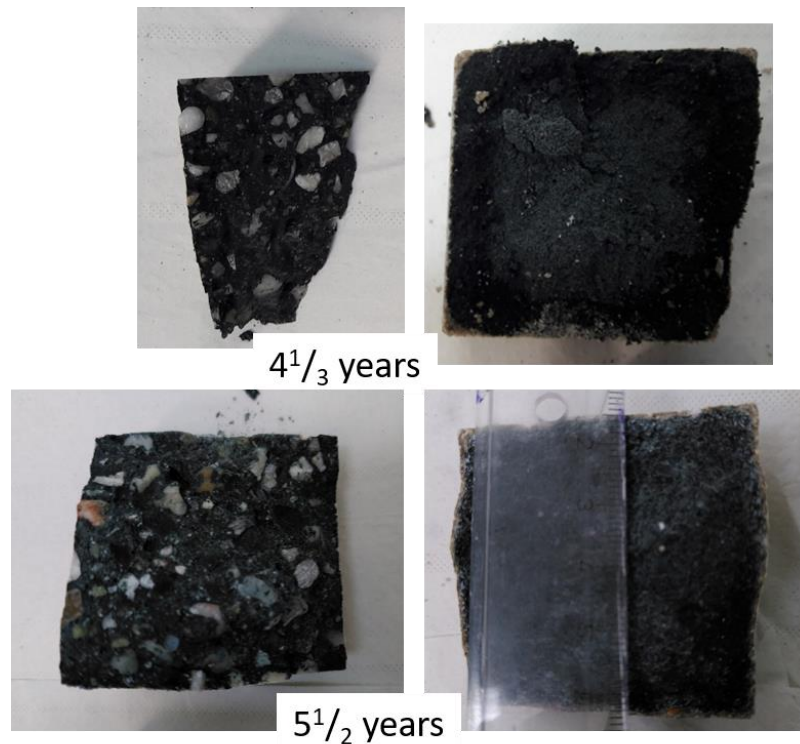
Figure 3-14: Oxidation at around room temperature after exposure to the saline solution in Table 3-5 for waste package and foamed concrete with CEM III/B of cubical specimens with an edge of 5 cm, all specimens sawn from a cubical specimen with an edge of 15 cm before this exposure

Figure 3-15: 'Oxidation" at around room temperature after exposure to the saline solution in Table 3-5 for foamed concrete with CEM I of a cubical specimen with an edge of 10 cm

EURAD (Deliverable n° 2.13) - **Intermediate level radioactive waste packages – Characterization of waste and backfill degradation experiments**
Dissemination level: Public
Date of issue of this report: **18/03/2024**

Page 35

3.5   Analysis of the leaching solutions

3.5.1 Preparation of samples

Only ICP-OES analysis of the samples exposed to a relative humidity of 98%, demineralised water and the saline solution in Table 3-5 were considered useful since sample preparation could only be performed at ordinary air conditions i.e. carbonation during sample preparation was considered highly likely. Pieces of mortar samples had been pulverized and aggregates were manually removed. Especially, the waste package concrete (13% porosity) was hard to pulverize. Usually cement pastes without sand and gravel are analysed in order to facilitate sample handling (e.g. Lothenbach et al. (2012)). Aggregates like sand and gravel or other siliceous additives are however used to manufacture almost any cementitious material for disposal of radioactive waste. Reaction rims between the aggregates and cementitious fluid are generated during hardening until thickening of a reaction rim of hydrates covers the external surface of the aggregate. The reaction is then slowed down considerably and proceeds through a diffusion controlled process (Jackson et al., 2017).

The resulting powder from the pulverization was dried at 105°C for 3 hours. Table 3-6 shows the loss in weight of the powders. In addition, cement (CEM III/B) used to manufacture waste package concrete was also dried.

Table 3-6: Loss in weight of powders

Environment	Type of concrete	Loss in weight (%)	Type of concrete	Loss in weight (%)
Relative humidity 98%	Waste package	4.7	Foamed	15.5
Demineralised water	Waste package	5.3	Foamed	16.4
Dutch clay pore water	Waste package	3.8	Foamed	11.9
Cement (CEM III/B 42.5 N LH/SR from ENCI)	0.19			

The procedure from NEN 7371 (Leaching characteristics – Determination of the availability of inorganic components for components – Solid earthy and stony materials for the dried powders) was used. This standard has a track record in obtaining reproducible results for inorganic components in fly ashes and other ashes, limestone and fired bricks and is required to determine whether the leaching of inorganic components takes place by diffusion according to NEN 7375. Hereto:

- A mass of 5 000 gram of powder was mixed with 250 ml demineralised water in a glass beaker;
- The pH was measured after 1 minute;
- A volume of 1 M HNO_3 was added to achieve a pH of 7 ($V_{1,a}$), additional 1M HNO_3 was added during stirring for 3 hours in order to keep the pH at 7 ($V_{1,b}$);
- The suspension was filtered; conductivity and temperature of the filtered solution (I) was acidified for conservation. This acidification was till a pH of 2 or lower and the acidified solutions were stored in polyethylene bottles for ICP-OES analysis;
- The left solid matter on top of the filter was rinsed in demineralised water, additional demineralised water was added until 250 ml was achieved;
- A volume of 1 M HNO_3 was added to achieve a pH of 4 ($V_{2,a}$), additional 1M HNO_3 was added during stirring for 3 hours in order to keep the pH at 4 ($V_{2,b}$);
- The suspension was filtered; conductivity and temperature of the filtered solution (II) was acidified for conservation. This acidification was till a pH of 2 or lower and the acidified solutions were stored in polyethylene bottles for ICP-OES analysis.

The temperature should remain between 18°C and 22°C according to NEN 7371. Table 3-7 shows that sometimes a slightly higher temperature than 22°C was measured.

In NEN-7371:2004, solution II needs to be analysed but solution I and II have been measured for this report. All elements (Na, Ca, K, Mg, Fe) in the solutions could be easily detected, the error in the measurements of the solutions was 5%.

EURAD (Deliverable n° 2.13) - **Intermediate level radioactive waste packages – Characterization of waste and backfill degradation experiments**
Dissemination level: Public
Date of issue of this report: **18/03/2024**

Page 36

3.5.2 Measurement of the solutions and determination of content

Table 3-7 and Table 3-8 shows the ICP-OES measurements obtained from the two solutions (I) and (II) of each powdered sample. According to NEN 7371:2004, the availability of each measured element in mg per kg dry matter can be determined through:

$$U_{avai} = \frac{c \times (2V_0 + V_1 + V_2)}{(m_0 \times f_1)}$$

where c is the concentration in solution II in µg/l, V_0 is the amount of demineralised water (250 ml), V_1 is the amount of added 1 M HNO_3 ($V_{1,a}+V_{1,b}$ in Table 3-7) to achieve a pH of 7, V_2 is the amount of added 1 M HNO_3 ($V_{2,a}+V_{2,b}$ in Table 3-7) to achieve a pH of 4, m_0 is the dried mass (5 000 gram) and f_1 is the conversion factor 1000 µg/g. Figure 3-16 shows the measured concentration according to this NEN norm. The values expected for cement have been determined with the producer specification in Table 3-2 for CEM III/B. Only a Na_2O equivalent is available for ECNI cement and therefore the speciation for HCM cement have been used to determine the expected values.
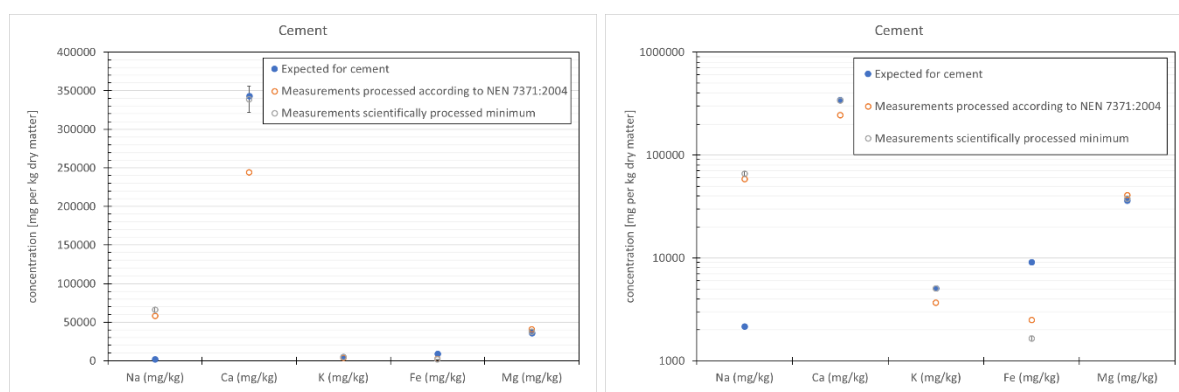
Figure 3-16: Determination of concentration in cement at a linear (left) and log (right) scale, Na and K expected values are uncertain

EURAD (Deliverable n° 2.13) - **Intermediate level radioactive waste packages – Characterization of waste and backfill degradation experiments**
Dissemination level: Public
Date of issue of this report: **18/03/2024**

Page 37

Table 3-7: ICP-OES measurements of solutions of concrete powders and cement; measurement error in solutions about 5%

Environment	Sample ID	Solution ID		T °C	Conductivity mS/cm		Na mg/l	Ca mg/l	K mg/l	Fe mg/l	Mg mg/l	$V_{1,a}$ (ml)	$V_{1,b}$ (ml)	$V_{2,a}$ (ml)	$V_{2,b}$ (ml)
					Meas.	Deter.[inf]									
Rel. hum 97.6%	HS_58_50	pH to 7 (I)	1	23.8	3.75	4.40	818	801	18	7	42	8.82	2.60		
		pH to 4 (II)	2	22.5	5.30	4.14	678	664	14	21	134			5.40	9.25
Demineralised water	HS_60_50	pH to 7 (I)	3	22.1	3.75	4.02	653	794	25	2	42	4.56	8.80		
		pH to 4 (II)	4	21.4	5.12	4.27	707	692	17	20	131			5.02	14.00
Dutch clay pore water	5_HS_80_50	pH to 7 (I)	5	21.6	-	4.69	786	884	11	4	74	5.63	9.47		
		pH to 4 (II)	6	20.9	5.05	3.88	644	567	10	16	163			4.41	13.75
Rel. hum 97.6%	COV50_39	pH to 7 (I)	7	21.6	4.69	4.61	576	1030	12	6	59	8.32	11.70		
		pH to 4 (II)	8	21.1	3.93	3.62	792	458	12	20	99			3.75	10.30
Demineralised water	COV50_43	pH to 7 (I)	9	21.5	4.05	4.72	752	951	10	5	50	7.69	10.17		
		pH to 4 (II)	10	22.1	4.10	3.55	710	486	10	23	104			4.85	10.76
Dutch clay pore water	7_COV_58	pH to 7 (I)	11	21.8	4.66	4.80	652	1060	10	3	47	7.56	11.41		
		pH to 4 (II)	12	21.9	3.70	3.16	647	423	9	18	95			3.59	9.60
Cement (CEM III/B)		pH to 7 (I)	17	23.1	12.7	10.3	446	2850	42	1	177	25.00	41.20		
		pH to 4 (II)	18	-	-	8.57	476	2000	30	20	334			11.10	33.70

ID = Identification, COV: waste package mortar (13% porosity) that COVRA uses for conditioning of the waste HS: foamed mortar (21% porosity); Meas.: measured, Deter.[inf] determined conductivity from the Na, Ca, K Fe and Mg content assuming infinite dilution at 25°C, - not registered.

Table 3-8: ICP-OES measurements of solutions; error in measurements about 5%

Concentration	Conductivity mS/cm Deter.	Na [mg/l]	Ca [mg/l]	K [mg/l]	Fe [mg/l]	Mg [mg/l]	Solution ID
Measured Dutch clay pore water exposed to concrete for $4\frac{1}{3}$ years	115.4	47100	274	800	50	2370	16
Expected Dutch clay pore water from Table 3-5 if no interaction with concrete	32.1 (79.4)	11164	425	407	4	1310	-
Demineralised water exposed to waste package concrete at 5°C for about 1000 days	0.24	64	17	25	0.076	1.06	13
Demineralised water exposed to waste package concrete at 20°C for about 1000 days	0.28	70	10	48	0.090	0.50	14
Demineralised water exposed to foamed concrete at 5°C for about 1000 days	0.31	94	13	36	0.072	0.16	15

Deter.[inf] determined conductivity from the Na, Ca, K Fe and Mg content assuming infinite dilution at 25°C, in brackets with all dissolved components i.e. including e.g. Cl^- and SO_4^{2-}.

EURAD (Deliverable n° 2.13) - **Intermediate level radioactive waste packages – Characterization of waste and backfill degradation experiments**
Dissemination level: Public
Date of issue of this report: **18/03/2024**

Page 38

Figure 3-16 clearly shows that too low calcium content is determined with the proposed formula in NEN 7371:2004. The scientifically determined content approaches more the expected calcium content and is determined by:

$$U_{avai} = \frac{c(I) \times (V_0 + V_1)}{(m_0 \times f_1)} + \frac{c(II) \times (V_0 + V_2)}{(m_1 \times f_1)}$$

where $c(I)$ is the concentration measured for the solution pH=7, $c(II)$ is the concentration measured for the solution pH=4 and m_1 is the mass left solid matter on top of the filter in obtaining the solution pH=7. The mass m_1 is not measured and therefore a value of 3.716 gram was determined from the Na, Ca, K, Mg and Fe content in solution I and oxide compositions. Al_2O_3 and SO_3 are also present in Table 3-2 and therefore this determined mass is overestimated. Therefore, minimum is added to 'scientifically processed'. The conductivity measurements could help to elucidate the missing components in the solution. The determined conductivity in Table 3-7 (and Table 3-8) is based on the measured elemental compositions; the addition of ml of 1M HNO_3 has a negligible effect on this determined conductivity. This exercise to deduce the missing components is tedious and would be speculative since the conductivity determined with the molar conductivity needs to be corrected with the interaction coefficients between the dissolved species and therefore not performed.

For the powders obtained from the pulverized samples, hydrated cement was used that could have been carbonated during the pulverization at ordinary air conditions. Hydration and carbonation of cement will both lead to a smaller measured concentration of Ca, Mg and Fe than pure cement. For Na and K, the effect is hard to determine since chemisorption of these elements takes place by cementitious minerals rather than incorporated in a cement mineral. Table 3-8 shows that both Na and K are enriched in the saline solution which can be attributed to the leaching of dissolved alkalis. The interpretation of the demineralised water exposed concrete requires an ICP-OES measurement of demineralised water that is not exposed. This measurement has not been done.

The aim during the pulverisation was to remove quartz aggregates but that is not possible for small sand grains. Figure 3-17 shows the expected concentrations of Ca, Fe and Mg if there would no interaction with demineralised or saline water.
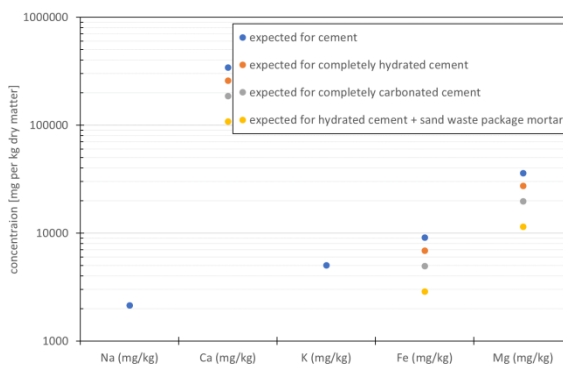
Figure 3-17: Expected concentrations if no interaction with demineralised or saline water

Figure 3-18, Figure 3-19 and Figure 3-20 show the interpretation analysis of the ICP-OES results for the concrete samples. The minimum value is determined by assuming $m_1 = m_0$ i.e. no mass loss in the first step (the preparation of solution I pH=7). The maximum value is determined by $m_1 = m_0 \times \text{sand}/_{(\text{sand+water+ cement})}$ i.e. all hydrated cement is lost in the first step. The assumed mineralogy of the hydrated cement is shown in the Initial SOTA of ACED for CEM III/B (Neeft et al., 2022).

The derived calcium concentration can be understood for foamed concrete and also for waste package concrete if not only sand but also a fraction of the aggregates was not removed during pulverisation, although the calcium concentration seems to be impoverished for the saline solution. Table 3-8 is presenting that both types of concrete show no difference between exposure to

EURAD (Deliverable n° 2.13) - **Intermediate level radioactive waste packages – Characterization of waste and backfill degradation experiments**
Dissemination level: Public
Date of issue of this report: **18/03/2024**

Page 39

demineralised water and saline water i.e. the exchange of calcium was too limited to measure an effect of exposure.
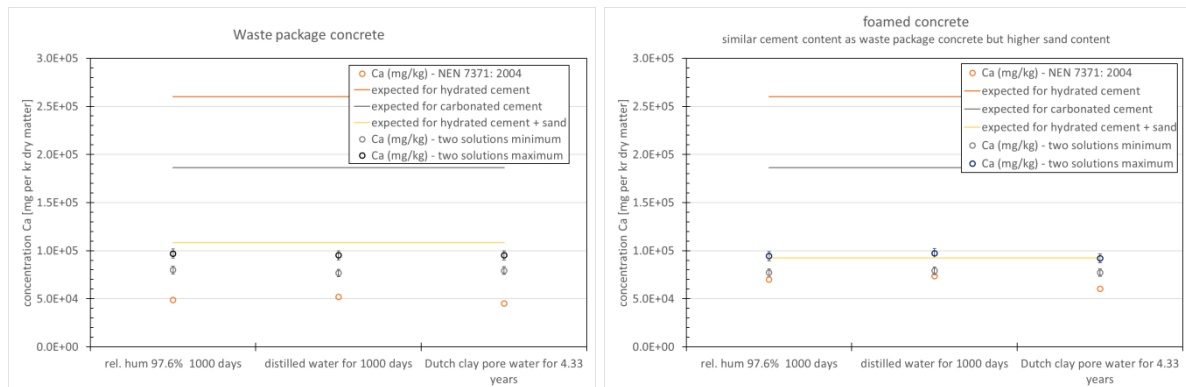
Figure 3-18: Measured calcium content; expected values without any interaction with demineralised or saline water

Foamed concrete seems to get enriched in magnesium in Figure 3-19 by exposure to the saline solution but the magnesium concentration Table 3-8 seems to be enriched as well. Waste package concrete shows no difference between exposure to demineralised water and saline water in Figure 3-19 i.e. the exchange of magnesium was too limited to measure an effect of exposure.
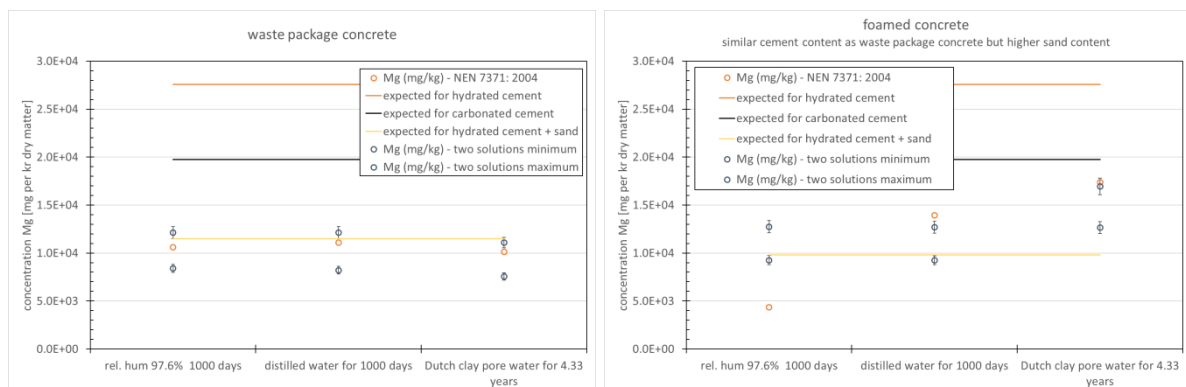
Figure 3-19: Measured magnesium content; expected values if no interaction with demineralised or saline water

The iron concentration seems to be enriched for the saline solution in Table 3-8 and both types of concrete may be slightly impoverished in iron but the iron concentration is always lower than expected (Fig. 20).

EURAD (Deliverable n° 2.13) - **Intermediate level radioactive waste packages – Characterization of waste and backfill degradation experiments**
Dissemination level: Public
Date of issue of this report: **18/03/2024**

Page 40
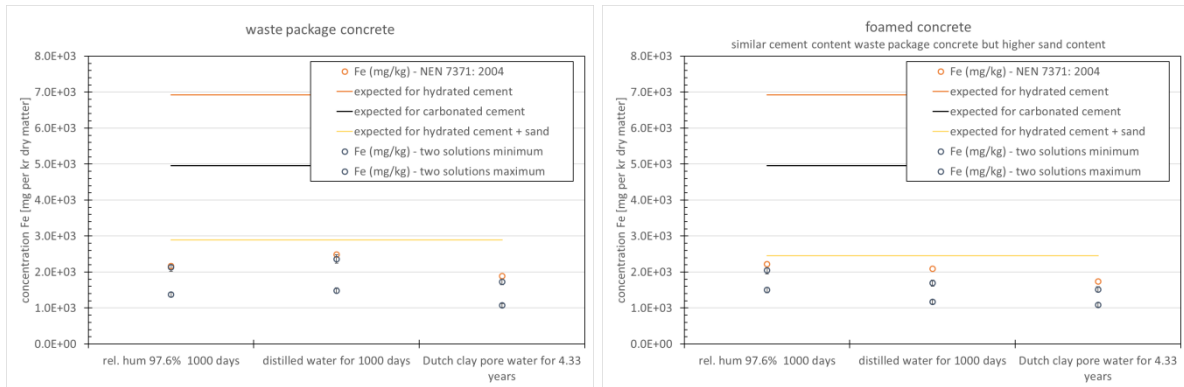
Figure 3-20: Measured iron concentration; expected values if no interaction with demineralised or saline water

3.5.3 Acid neutralizing capacity

According to NEN 7371: 2004, an indication of the acid neutralizing capacity (ANC) can be determined with:

$$ANC_{pH:7} = \frac{V_1 \times c_1^{HNO3} \times f_2}{m_0} \quad \& \quad ANC_{pH:4} = \frac{\left(V_1 \times c_1^{HNO3} + V_2 \times c_2^{HNO3}\right) \times f_3}{m_0}$$

where c_1^{HNO3} and c_2^{HNO3} are the molar concentrations of added nitric acid in the first and second step, f_2 and f_3 are conversion factors, both 1 l×g/ml×kg. The capacity of the large volume of demineralised water is then not included. This additional capacity is only a slight contribution to the total capacity and only in the determination of $ANC_{pH:7}$. The negligence of the loss is mass in step 1 is envisaged to have a larger impact, especially for cement. For cement: $ANC_{pH:7}$ is 13.24 mol/kg dry matter according to NEN and 13.27 mol/kg dry matter if the rise in pH in demineralised water in Table 3-7 is included and the waste dissociation constant at 25°C is assumed. $ANC_{pH:4}$ is 22.20 mol/kg dry matter using NEN 7371:2004 and 29.87 mol/kg dry matter if the mass loss in the first step would be included i.e. m_0 should be m_1. Figure 3-21 clearly shows that the acid neutralizing capacity for pulverized powder obtained from waste package concrete is larger than for foamed concrete. A difference attributed to the exposing environment can, however not been observed for waste package concrete e.g. if the ANC at pH=7 is somewhat higher than the ANC at pH=4 is somewhat lower. Foamed concrete seems to show differences that may be attributed to the exposing environment. Figure 3-21 shows that the highest ANC for foamed concrete is measured for samples exposed to saline water.
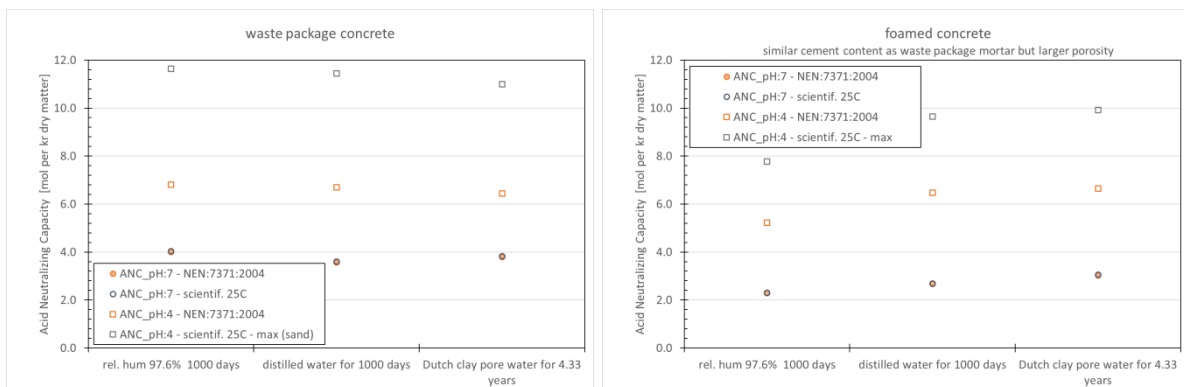
Figure 3-21: Acid neutralizing capacity for waste package concrete and foamed concrete. ANC_pH:4 - NEN:7371:2004 is also minimum for scientifically processed data

EURAD (Deliverable n° 2.13) - **Intermediate level radioactive waste packages – Characterization of waste and backfill degradation experiments**
Dissemination level: Public
Date of issue of this report: **18/03/2024**

Page 41

3.5.4 Concluding perspective and recommendations

The elemental concentration of concrete i.e. cementitious materials with aggregates, and the solutions to which they have been exposed have been measured. Although the pulverisation of concrete could only be performed in ordinary air, the cementitious materials were not completely carbonated i.e. there is still some acid neutralisation capacity in the samples, for waste package concrete more than foamed concrete. The saline solution was enriched in dissolved alkalis that may result from the leaching of concrete. Leaching of calcium has not been observed for both types of concrete. Foamed concrete seems to show a difference that may be attributed to the exposure environment i.e. enrichment in magnesium due to exposure of the saline solution and reduction in acid neutralization capacity due to exposure to air. The measurements of the concentration of magnesium and iron of both in the solution and concretes are, however, not yet understood. Additional chloride and sulphate measurements could help to understand these measurements.

NEN 7371:2004 was used as the methodology to determine the availability of the elemental components. In this NEN 7371:2004 two solutions are prepared but the loss of the mass in the first prepared solution becomes unknown. Another methodology is dissolving a sample in acid by which a single solution is obtained. In (Lothenbach et al., 2012), a 3% HCl solution is used for cement. A HNO_3 solution would be better to see the effect of interaction with saline solutions.

Pulverisation of concrete samples is quite difficult especially waste package concrete that COVRA manufactures for conditioning of the waste. Exposing a weighted piece of concrete to an acid solution HNO_3 and waiting until aggregates are left may be a more convenient methodology to measure the elemental concentration of concrete. The measurement of the solid mass left on the filter would provide the missing information how much mass was dissolved in the acid.

3.6   Other test and characterisations

3.6.1 Porosity and water retention

The porosity has gravimetrically determined to be 12-13% for waste package concrete and 24-25% for foamed concrete made with CEM III/B (Mladenovic et al., 2019). At that time, it was difficult to account for the difference in weight between the samples exposed to the highest relative humidity and distilled water. The relative humidity determines the liquid pressure through the Kelvin-Laplace equation e.g. Poyet (2016) and Schneider et al. (2012):

$$P_{liquid}(RH, T) = -\rho_{water}(T) \frac{RT}{M_{H_2O}} \ln \left(\frac{RH}{100} \right)$$

where $\rho_{water}(T)$ is the density of water as a function of temperature, R is Boltzmann constant, T is temperature and M_{H2O} is the molar mass of water. The difference between liquid pressures is negligible between the samples exposed to the highest relative humidity's. The difference in weight between the samples exposed to the highest relative humidity and demineralized water is therefore rather related to incomplete drying of the surfaces of the samples exposed to this water then a bulk specific property. This different interpretation has an impact on the determination of the porosity of foamed concrete manufactured with CEM III/B i.e. that is now assumed to be 20-21% (Neeft et al., 2021) instead of 24-25% (Mladenovic et al., 2019).

The liquid pressures at a relative humidity of 6% at 20°C are so high i.e. 380 MPa that it is assumed that there is no liquid water is present sample. The figures of the carbonation rims in section 3.4.1.4 are very small and iron is present in trace amounts. It is therefore assumed that the difference in weight at start of exposure until after about 1000 days therefore is solely attributed to the loss in water. This difference in weight divided by density of water provides the volume of water that is released. The porosity is then determined by the volume of water divided by the volume of the specimen. The

EURAD (Deliverable n° 2.13) - **Intermediate level radioactive waste packages – Characterization of waste and backfill degradation experiments**
Dissemination level: Public
Date of issue of this report: **18/03/2024**

Page 42

smaller loss in weights measured from the other samples is assumed to be water volume in the sample that is in equilibrium with the exposed relative humidity. This water retention is usually fitted e.g. Schneider et al. (2012) and Poyet (2016) through the following equation (van Genuchten, 1980):

$$w = w_r + \frac{(w_s - w_r)}{[1 + (\alpha h)^n]^m}$$

where w is the volume of water content per total volume, w_r is the residual water volume per total volume, w_s is the saturated water volume per total volume, α and n are empirical parameters and m=1-$^1/_n$. In this report, w_r has been taken 0, w_s is the porosity and the Genuchten parameter n has been taken to be independent of the temperature for the fitting. The so-called alpha-parameter is a kind of suction force. Suction forces are temperature dependent and therefore α is assumed to be temperature dependent. Figure 3-22 shows the experimental results and the fitting lines with the parameters presented in Table 3-9. Closed symbols are results of samples that have been permanently exposed to the relative humidity i.e. there was always salt observed in the solution with which the relative humidity was obtained. Open symbols are results of samples may not always been exposed to a relative humidity i.e. the salt was completely dissolved by which it is assumed that the salt solution had become unsaturated.

Table 3-9: Genuchten parameters determined with a best fit by the eye

Type of concrete	w_s vol%	w_r vol%	temperature-independent		α (20°C)		α (5°C)	
			n	m	m^{-1}	Pa^{-1}	m^{-1}	Pa^{-1}
Waste package mortar	13	0	2.0	0.50	2.0×10^{-4}	2.0×10^{-8}	1.5×10^{-4}	1.5×10^{-8}
Foamed concrete	21	0	1.7	0.41	8.2×10^{-4}	8.2×10^{-8}	2.0×10^{-4} 3.0×10^{-4}	2.0×10^{-8}

EURAD (Deliverable n° 2.13) - **Intermediate level radioactive waste packages – Characterization of waste and backfill degradation experiments**
Dissemination level: Public
Date of issue of this report: **18/03/2024**

Page 43
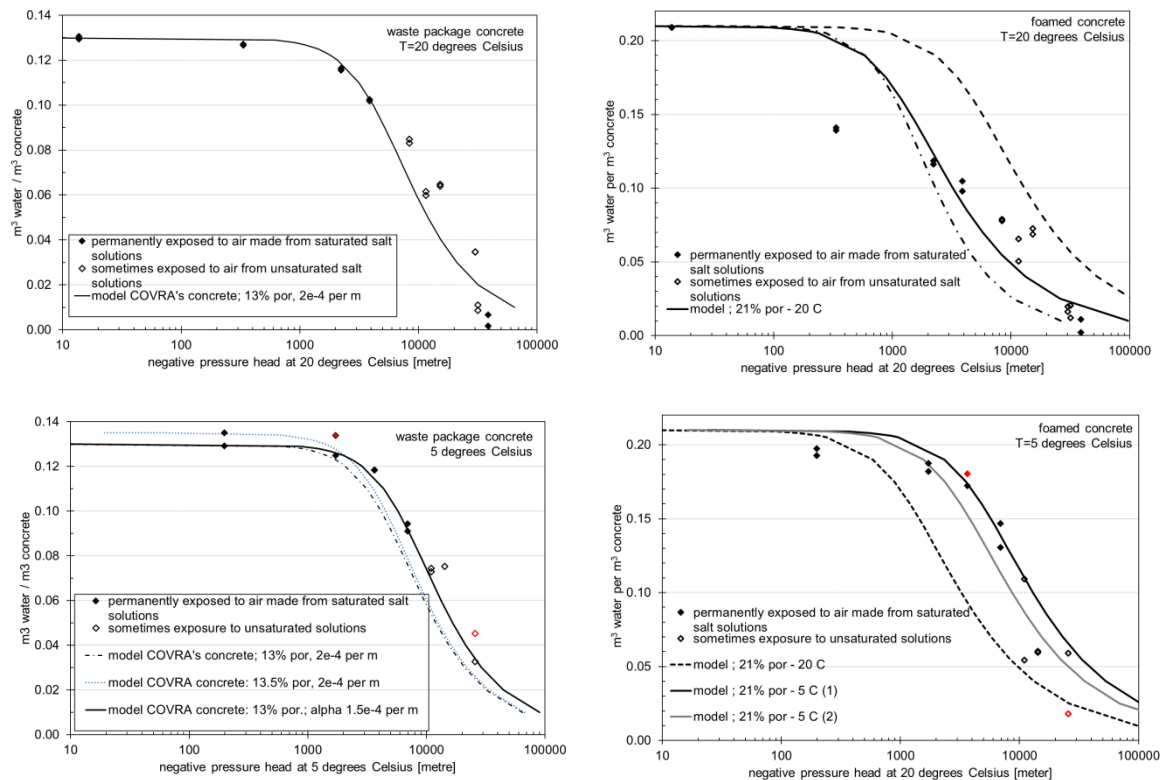
Figure 3-22: Determination of the Genuchten parameters for the waste package concrete and foamed concrete made with CEM III/B assuming $w_r=0$ from experimental results exposed to relative humidity's for about 1000 days. Samples on which salt had been observed on the surface are marked red.

The van Genuchten relation for water retention can also be used for the studied concretes, except for an outlier at 20°C at a negative pressure head of 335 metres i.e. a relative humidity of 98%. The range in negative pressure head (or relative humidity) in Figure 3-22 is quite large compared to published experimental values for concrete. For example, Schneider et al. (2012) used an experimental range between 300 metres and 3000 metres at 21°C and Poyet (2016) has found experimental values for concrete in a range between a relative humidity of 50% and 100%.

There is limited data about the temperature dependency of water retention curves. To our knowledge only Poyet (2016) has retrieved the temperature dependency of the water retention but in cement pastes, except that w_s i.e. porosity had not been derived from the experimental results he had found. Only analysis of data like presented in Figure 3-23 for the two types of investigated concrete is available in his study. Another difference with the current study is that he assumes a temperature dependency for m and α (see Table 2 in Poyet (2016)).

EURAD (Deliverable n° 2.13) - **Intermediate level radioactive waste packages – Characterization of waste and backfill degradation experiments**
Dissemination level: Public
Date of issue of this report: **18/03/2024**

Page 44
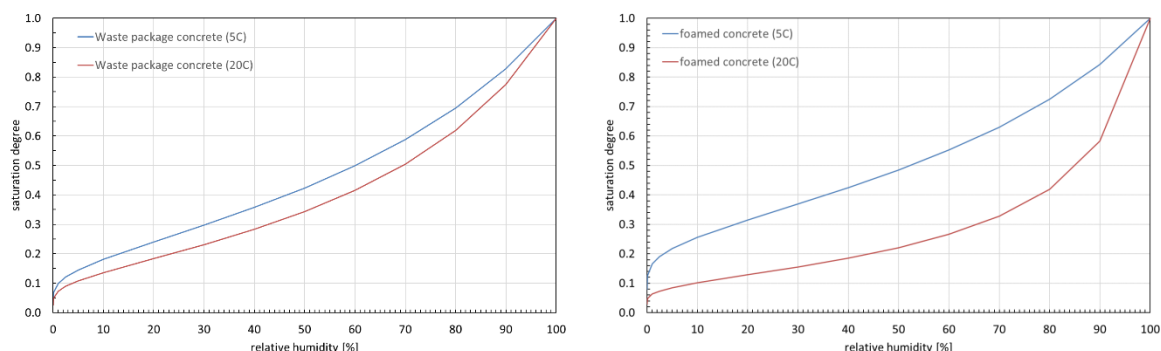
Figure 3-23: Genuchten parameters with saturation degree for the two types of concrete

3.6.2 Distribution in size of pores

The liquid pressure can also be viewed as a capillary pressure through Young-Laplace's equation e.g. NAGRA (2008):

$$P_{cap} = \frac{2 \times \sigma_{g-l}(T) \times \cos\theta}{r}$$

where σ_{g-l} is the surface tension across the pore water gas interface which is $72.74{\times}10^{-3}$ N/m at 20ºC and $74.94{\times}10^{-3}$ N/m at 5ºC[1] (Lemmon, 2015), Θ is the contact angle between the water-gas interface and the solid material which is approximately 0 degrees for water-air-concrete. The differential volume in Figure 3-22 provides the occurrence of the pores with a certain diameter. This approach is usually not performed e.g. Poyet (2016) and Schneider et al. (2012) but is included in this report.

The water content within the sample exposed to a relative humidity of 6% at 20°C in pores with a radius of 0.38 nm is assumed to be 0 and a relative humidity of 99.9% at 20°C pore with a radius of 1000 nm is assumed to be saturated. This relative humidity is assumed to be achieved by wet cotton and therefore not included in the range of Figure 3-24. The water content at 5°C is determined by using the porosity determined by the water loss at a relative humidity of 6% at 20°C as a start since only higher relative humidity's are available for the series exposed at 5°C.

For waste package concrete, the distribution in size of pores determined at 20°C is almost similar to this distribution of pores at 5°C except that the water content at lower relative humidity in smaller radii is more prominent at 5°C than at 20°C. Waste package concrete did not lose water at 98% at 20°C but foamed concrete did, see the outlier in Figure 3-22 at 335 metres. That's why the differential volume is still increasing with increasing radius at 20°C. At 5°C, there is no outlier in Figure 3-22 for foamed concrete and the behaviour is similar to waste package concrete except that the differential volume of pores is larger and the predominance is of a larger size in pores. For the waste package concrete, the increasing measured compressive strength of the samples could be explained by the larger capillary (suction) force induced by the decreasing equilibrium moisture content with decreasing relative humidity by assuming no difference in the distribution in the size of pores (Neeft et al., 2021).

---

[1] The value at 5ºC is determined by the average of the surface tension at 4ºC of 75.08 mN/m and 74.80 mN/m at 6ºC.

EURAD (Deliverable n° 2.13) - **Intermediate level radioactive waste packages – Characterization of waste and backfill degradation experiments**
Dissemination level: Public
Date of issue of this report: **18/03/2024**

Page 45
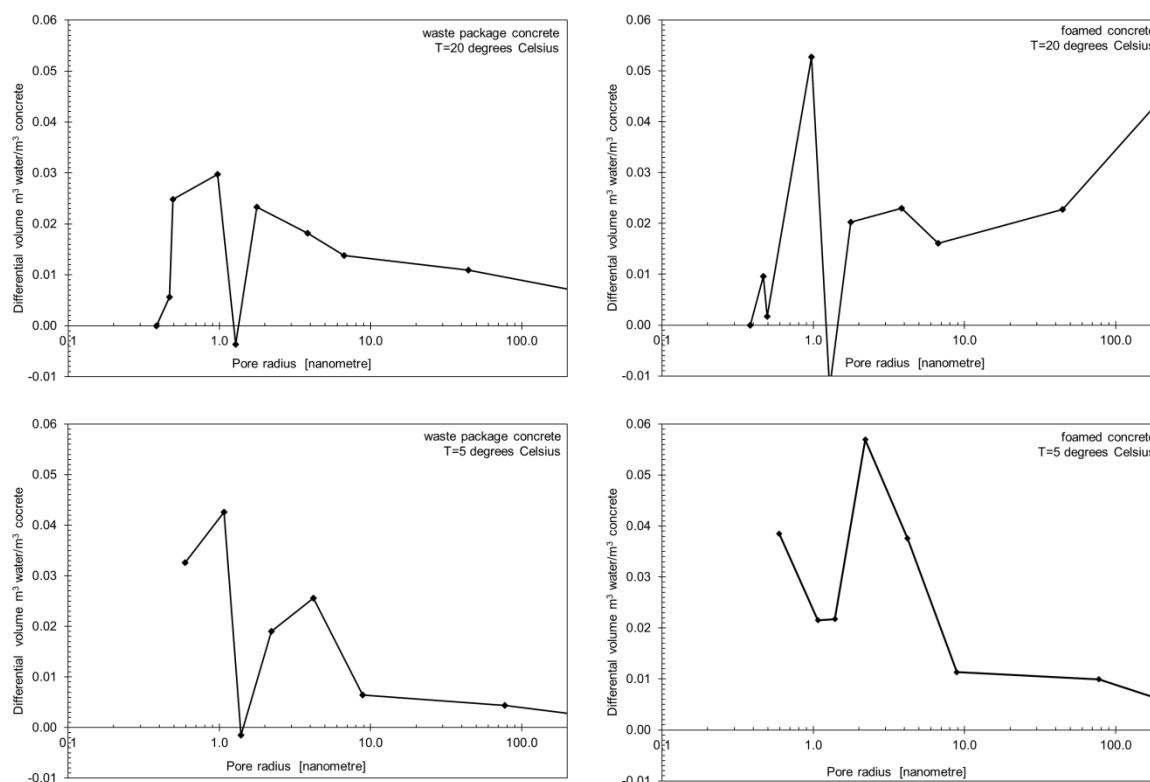
Figure 3-24: Distribution of pores determined by water retention curves.

In the paper by Poyet (2016), for same type of cement i.e. CEM I and CEM V/A, cement pastes have a lower saturation degree than concrete at similar relative humidity's. As the equilibrium content is independent of the size of the sample, it is therefore very cautiously proposed here that cement paste has relatively larger size in pores than concrete made with the same type of cement. The reaction rims made during hardening between the aggregates and cementitious fluid (Jackson et al., 2017) may provide a denser and more refined pore structure than cement paste alone.

3.6.3 Water saturated permeability

Poyet (2016) also came with permeability values for the experimental values obtained from literature for cement paste i.e. at 293.15 K for paste made with CEM I 12.2×10^{-23} m^2 and with CEM V/A $\approx7\times10^{-23}$ m^2. For the two types of investigated concrete with CEM III/B, it is assumed that the saturated permeability depends on the porosity as well as the radius of the pores (Millington and Quirk, 1961):

$$K_{sat} = \frac{1}{8}w_s r_c^2$$

where r_c is the characteristic radius determined by the Young-Laplace equation using the reciprocal of the Genuchten parameter α as the characteristic pressure. This pressure is also called apparent air entry pressure (NAGRA, 2008). Table 3-10 shows that those determined permeability values are more than two orders in magnitude larger than determined by Poyet (2016) for cement paste. Cement paste is usually considered the part of concrete that contributes most to the porosity and therefore the investigated concretes are envisaged to have a smaller permeability than cement paste. There is however also other data available. An intrinsic permeability of 10^{-19} m^2 is suggested for waste package concrete and high performance concrete, both with a porosity of 15% in the compilation made by the

EURAD (Deliverable n° 2.13) - **Intermediate level radioactive waste packages – Characterization of waste and backfill degradation experiments**
Dissemination level: Public
Date of issue of this report: **18/03/2024**

Page 46

Swiss waste management organisation (NAGRA, 2008). This suggested value is similar to the value shown in Table 3-10 at 20°C.

COVRA's waste package concrete is impermeable for engineering purposes as explained in section 3.1 but for geological disposal even the smallest permeabilities - negligible for engineering - need to be taken into account for the chemical evolution of disposal cells.

Table 3-10: Permeability with Genuchten parameters with Millington-Quirk

Type of concrete	Porosity / w_s vol%	w_r vol%	$1/\alpha$ (MPa)		r_c (nm)		K_{sat} (m^2)	
			20°C	5°C	20°C	5°C	20°C	5°C
Waste package mortar	13	0	49	65	3.0	2.3	7.3×10^{-20}	4.6×10^{-20}
Foamed concrete	21	0	12	49	12	3.1	2.2×10^{-18}	1.5×10^{-19}

EURAD (Deliverable n° 2.13) - **Intermediate level radioactive waste packages – Characterization of waste and backfill degradation experiments**
Dissemination level: Public
Date of issue of this report: **18/03/2024**

Page 47

4. Experiment 3: Investigation of concrete from the old hydroelectric power plant dams

Partners: ZAG, PSI

Contact person: Ana Mladenovic (ZAG)

Work performed by: Georg Kosakowski, Rainer Dähn, Guoqing Geng (PSI), Alojz Bevc, Pavel Zvanut, Ana Mladenovic (ZAG)

4.1 Field investigation of concrete from the old hydroelectric power plant dams

In order to get insight into a long-term aggregate reactivity in concrete structures and thus try to overcame the difficulties in simulating the long term alkali-aggregate reaction (AAR) damage in a structure with short term laboratory test and the translation of the test results to the actual structures, 10 boreholes have been drilled out at three hydroelectric power plant dams. Such data is essential to assess scenarios for ILW and HLW that consider internal degradation of concretes/mortars due to ASR. The selected dams are Fala hydroelectric power plant, Ozbalt hydroelectric power plant and Mariborski otok hydroelectric power plant. All structures are located on the Drava River in the north-east of Slovenia (Fig. 4-1). No historical records of the structures are available; however it is very likely that the plain cement was transported from the Trbovlje cement plant (established in 1873).

A climate in this area is a typical European continental influenced climate with warm, dry summers and fairly cold winters with snow and frequent fog. In summer, there can be short heat waves, with peaks of 35 °C. The average annual temperature is 9.5°C. The average annual rainfall is 986 mm.
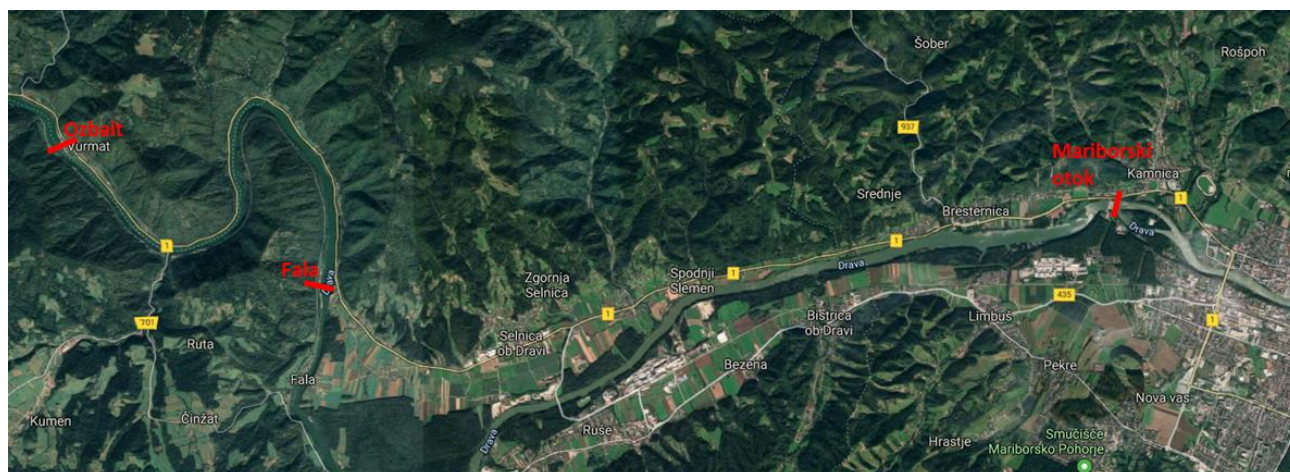
Figure 4-1: Location of the selected hydroelectric power plants on the Drava River

The Fala hydroelectric power plant

The Fala hydroelectric power plant is the fifth power plant in the Slovene section of the Drava River Chain and is the oldest hydroelectric power plant in this section (Fig. 4-2). Its construction began in 1913, with the first five units commissioned in 1918. The sixth unit was built in 1925 and a seventh in 1932. The reservoir has a length of 8.6 km and contains 4.2 million m^3 of water, of which 0.9 million m^3 can be used for the generation of electric power. The dam was originally built as a structure with five

EURAD (Deliverable n° 2.13) - **Intermediate level radioactive waste packages – Characterization of waste and backfill degradation experiments**
Dissemination level: Public
Date of issue of this report: **18/03/2024**

Page 48

spillways (each with a width of 15 m) allowing for the complete raising of individual groups of spillway gates.

Figure 4-2: The Fala hydroelectric power plant (source: http://www.dem.si/en-gb/Power-plants-and-generation/Power-plants/Fala-HPP)

The Ozbalt hydroelectric power plant

The Ozbalt hydroelectric power plant, with pier-type structure, is the fourth power plant in the Slovene section of the Drava River (Fig. 4-3). It was built between 1957 and 1960. The damming of the Drava River here resulted in a 12.7 km long reservoir containing 10.5 million m^3 of water, of which 1.4 million m^3 can be used for the generation of power. The dam structure itself is made up of three turbine piers placed between four spillways and the left and right bank buildings. The spilling capacity of all four spillways is 5800 m^3/s.

Figure 4-3: The Ozbalt hydroelectric power plant (source: http://www.dem.si/en-gb/Power-plants-and-generation/Power-plants/O%C5%BEbalt-HPP)

The Mariborski otok hydroelectric power plant

EURAD (Deliverable n° 2.13) - **Intermediate level radioactive waste packages – Characterization of waste and backfill degradation experiments**
Dissemination level: Public
Date of issue of this report: **18/03/2024**

Page 49

This hydroelectric power plant is located near city Maribor, exploiting the energy potential of the Drava River between the Fala hydroelectric power plant and the island on the Drava River (Fig. 4-4). The construction of the power plant had been planned prior to the World War II, but construction only began in 1942. The war caused the construction process to be drawn out considerably so that in May 1945 it was still only 30% completed. In 1948 the commissioning of the first unit was announced, with the second and third units beginning operation in 1953 and 1960. The dam has a 15.5 km long reservoir which contains 13.1 million m^3 of water. The dam structure contains three turbine piers placed between four spillways (each 18.75 m wide) and a left and right bank building. These spillways, closed by the double plate hook gates, have a total spilling capacity of up to 5600 m^3/s.

Figure 4-4: The Mariborski otok hydroelectric power plant (source: http://www.dem.si/en-gb/Power-plants-and-generation/Power-plants/Mariborski-otok-HPP)

4.1.1 Assessment of the structures

Regular monitoring (deformation measurements and visual inspections) has been established on all hydroelectric power plants on the Drava River Chain system. Monitoring has been established in 1970 for the Fala hydroelectric power plant, for the Ozbalt hydroelectric power plant in 1968 and for the Mariborski otok hydroelectric power plant in 1969. All degradation issues (delamination of the concrete, cracks, other damages) which could affect the durability or safety of the concrete structure are solved regularly.

4.1.2 Sampling

The sampling from the concrete structures have been performed in accordance to the Sampling Plan, which was prepared on a basis of results obtaining during the regular monitoring of the dams on the Drava River. A drilling machine with a diamond crown of diameter 100 mm was used. The length of the samples was up to 25 cm. Cores have been taken in different exposure environments in areas where cracking was suspected caused by ASR e.g. map cracking, longitudinal cracks or surface exudations. Sampling was carried out in September and November 2019 by ZAG, according to Godart et al (2013) and Jensen (1993). Sufficient precautions were taken during core sampling and subsequent sample preparation to ensure that evidences of ASR are retained. The selected data on the sampling is presented in Table 4-1.

Table 4-1: The selected data on sampling

EURAD (Deliverable n° 2.13) - **Intermediate level radioactive waste packages – Characterization of waste and backfill degradation experiments**
Dissemination level: Public
Date of issue of this report: **18/03/2024**

Page 50

	Age of concrete	Number of boreholes	Location
Fala hydroelectric power plant	105 years	4	indoor
Ozbalt hydroelectric power plant	62 years	4	outdoor
Mariborski otok hydroelectric power plant	74 years	2	indoor

Sampling of concrete at the Fala hydroelectric power plant

Four boreholes, designated as F1, F2, F3 and F4 have been drilled. Three sampling locations (F1, F2 and F3) were located in the "oil corridor" (Fig. 4-5), where the relative humidity is between 70% and 80%. Sample F4 has been taken from concrete in the "control corridor", where relative humidity is above 90% (Figs. 4-6 and 4-7). Both corridors are situated in the old part of a dam, built in 1918.
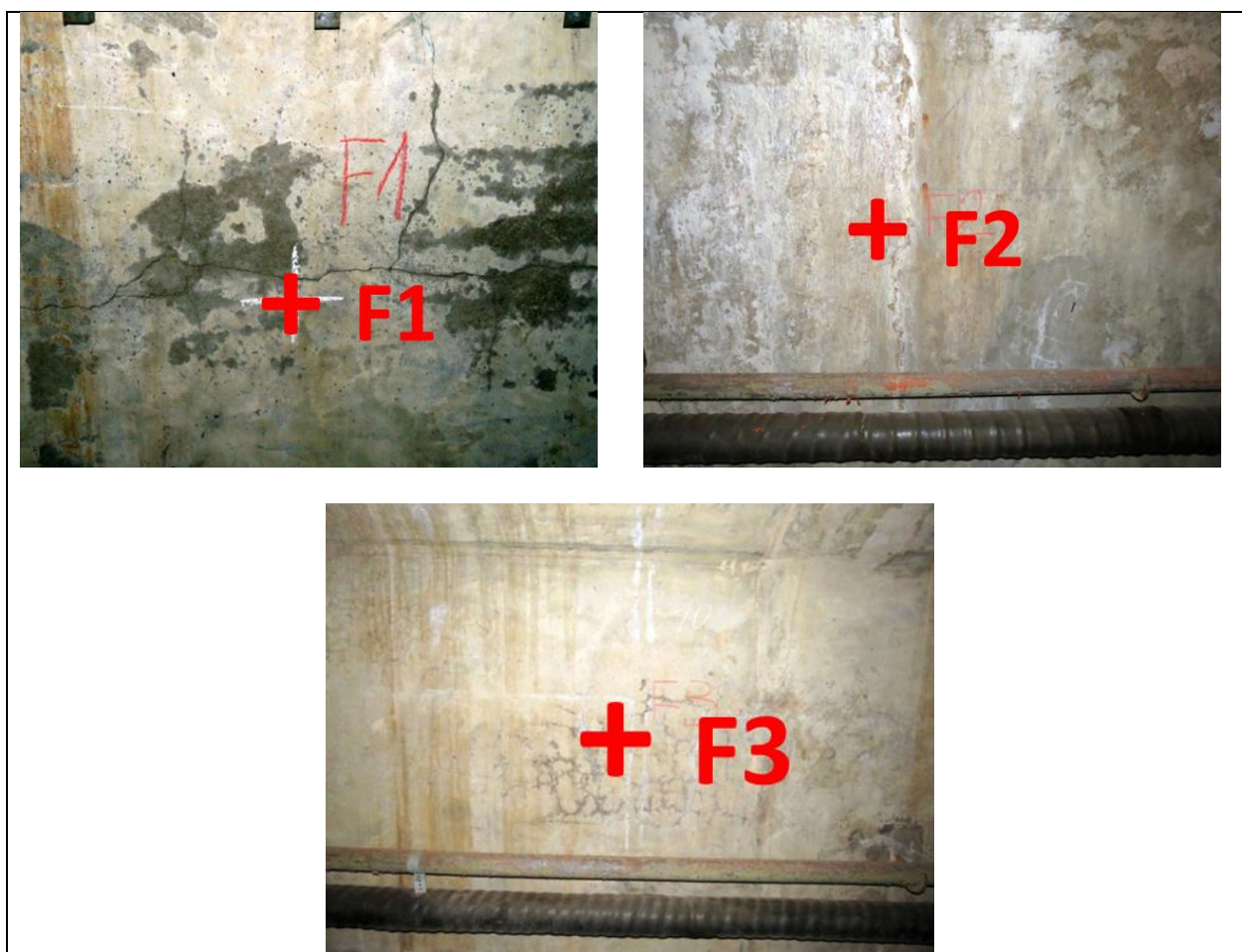
Figure 4-5: Location of the boreholes F1, F2 and F3 in the "oil corridor"

EURAD (Deliverable n° 2.13) - **Intermediate level radioactive waste packages – Characterization of waste and backfill degradation experiments**
Dissemination level: Public
Date of issue of this report: **18/03/2024**

Page 51

Figure 4-6: The "control corridor"

Figure 4-7: Location of the borehole F4 in the "control corridor"

Sampling of concrete at the Ozbalt hydroelectric power plant

Four boreholes, designated as V1, V2, V3 and V4 have been drilled out outdoor, V1 and V2, on the bridge with crane rail (Figs. 4-8, 4-9, and 4-10), and V3 and V4 on the third turbine pier (Fig. 4-11). Samples V1 and V2 have been drilled out at the location of the random cracks filled with white and yellowish exudations and precipitation. Intensive surface discoloration has been observed. Samples V3 and V4 are in the area where surface rehabilitation has been recently carried out and has therefore no visual cracks.

EURAD (Deliverable n° 2.13) - **Intermediate level radioactive waste packages – Characterization of waste and backfill degradation experiments**
Dissemination level: Public
Date of issue of this report: **18/03/2024**

Page 52

Figure 4-8: Concrete bridge with the crane rail

Figure 4-9: Location of the borehole V1

Figure 4-10: Location of the borehole V2
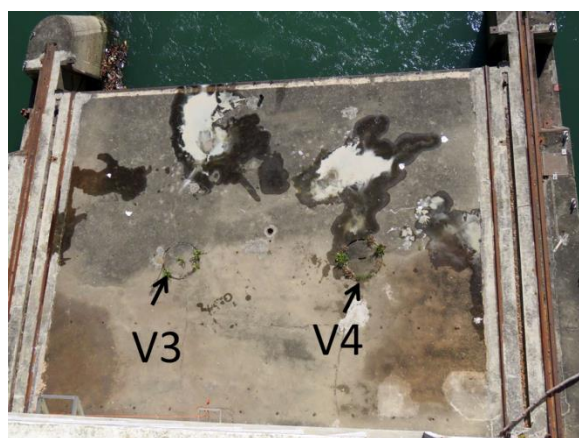
Figure 4-11: Location of the boreholes V3 and V4 on the third turbine pier

EURAD (Deliverable n° 2.13) - **Intermediate level radioactive waste packages – Characterization of waste and backfill degradation experiments**
Dissemination level: Public
Date of issue of this report: **18/03/2024**

Page 53

Sampling of concrete at the Mariborski otok hydroelectric power plant

Two boreholes, designated as M1 and M2 have been drilled out in the storage room, with an average relative humidity 60 % (Figs. 4-12 and 4-13).

Figure 4-12: Location of the borehole M1
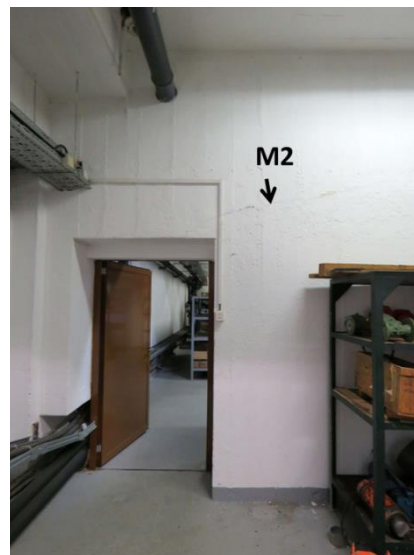
Figure 4-13: Location of the borehole M2

4.1.3   Laboratory investigation

Visual inspection

Visual inspection using a low power stereo microscope revealed the same type of aggregates in all samples of concrete which was a mixture of siliceous and carbonate sand and gravel, up to 32 mm in dimension. The grains are semi-rounded to rounded. The main components are quartz, quartzite, sandstone, siltstone, gneiss and amphibolite, as well as limestone and dolomite. This type of siliceous aggregates is considered as a slow-reacting aggregate. The mass ratio between siliceous and carbonate aggregate is approximately 60:40. The concrete samples from the Fala hydroelectric power plant are nonhomogeneous, porous, with large voids, cavities and parts where the cement matrix has been leached out (Fig. 4-14). The concrete samples from the Ozbalt hydroelectric power plant are much more homogeneous, well compacted, with low porosity and good contact between aggregate and matrix (Fig. 4-15). Similar characteristics have been revealed on the samples from the Mariborski otok hydroelectric power plant (Fig. 4-16). No clear signs of ASR reaction in term of rims, gel exudations or cracks have been observed during the macroscopic examination.

EURAD (Deliverable n° 2.13) - **Intermediate level radioactive waste packages – Characterization of waste and backfill degradation experiments**
Dissemination level: Public
Date of issue of this report: **18/03/2024**

Page 54

Figure 4-14: A sample from the Fala hydroelectric power plant (a core with entrapped air)

Figure 4-15: A sample from the Ozbalt hydroelectric power plant

Figure 4-16: A sample from the Mariborski otok hydroelectric power plant

4.1.3.1   Microscopic examination

4.1.3.1.1   Investigation of old concrete samples with SEM/EDS

The morphology and microstructure of the concrete mixtures were analysed on polished specimens in the transverse direction, in the JEOL 5500 LV SEM and JEOL JSM-IT500, which were coupled to an Oxford energy dispersive spectrometer, using backscattered electrons and a low vacuum. Examination of fractured samples has also been performed. The aim of these laboratory tests was to assess the degree of ASR in the concrete samples and the extent of this reaction.

The analysis focused mainly on the samples from the oldest dam (the Fala hydroelectric power plant), although the samples from other two locations were also examined. In this deliverable the main results from investigation on all three dams are presented.

ARS is present in all analysed concrete cores; although there is slight variation in intensity of reaction within each specimen, which is related to the porosity of the concrete. Parts with higher porosity are more affected.

Concrete samples from the Fala hydroelectric power plant

The signs of reaction are clear and involve both coarse and fine aggregate particles. Internal cracks, mostly in quartz, quartzite and gneiss are the most distinguish parameter of degradation. ASR occurs

EURAD (Deliverable n° 2.13) - **Intermediate level radioactive waste packages – Characterization of waste and backfill degradation experiments**
Dissemination level: Public
Date of issue of this report: **18/03/2024**

Page 55

in different forms. The most frequent features are micro cracks in quartz grains (Figs. 4-17 – 4-20). Grains of quartzite and gneiss are cracked along its grain boundaries. Cryptocrystalline reaction products in reacted aggregates have been identified in few cases (Figs. 4-21 and 4-22). Typical lime-alkali-silica gels or pure gels have not been observed. Some grains of quartz aggregate are shown in Figure 23, where it can be seen that the grains are cracked but have sharp, straight edges. All samples show a distinct crack pattern including radial cracks running from aggregates into the hardened cement paste (Figs. 4-24 – 4-26). Some cracks also cut the quartz grains or run along boundary between the cement matrix and the grains. The contact between the siliceous grains and the cement paste is poor (Fig. 4-27), and at the interface relatively high porosity occurs as a result of ASR (Fig. 4-28).
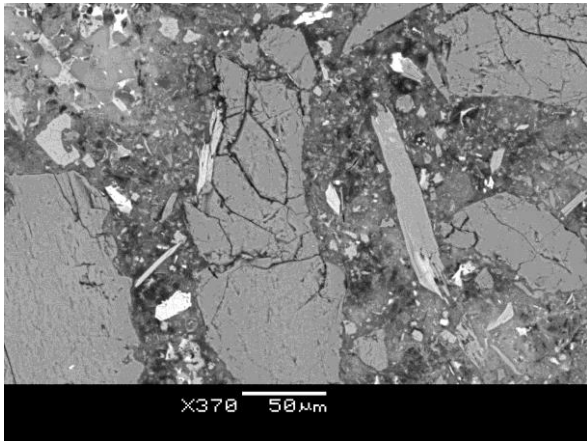
Figure 4-17: Cracks in quartz aggregate (the Fala dam)
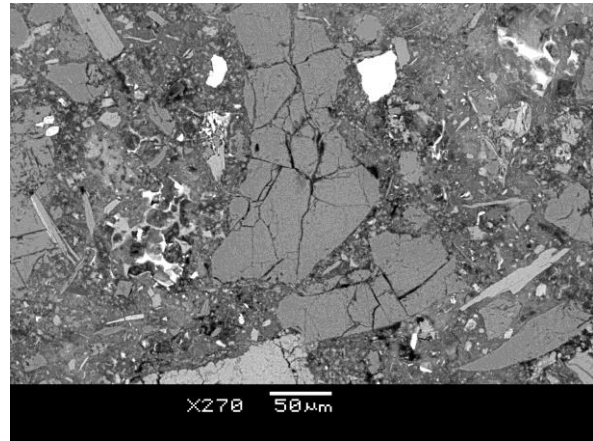
Figure 4-18: Cracks in quartz aggregate
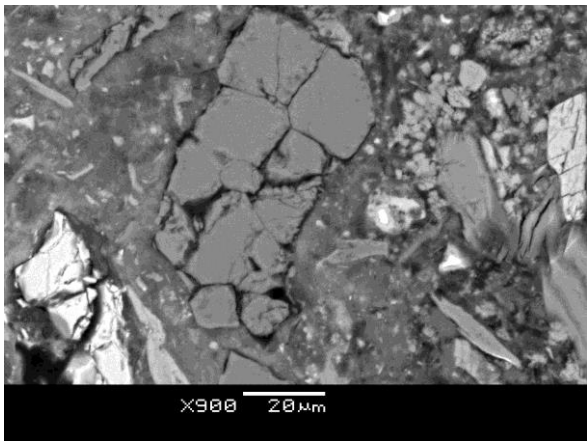
Figure 4-19: Cracks in quartzite aggregate
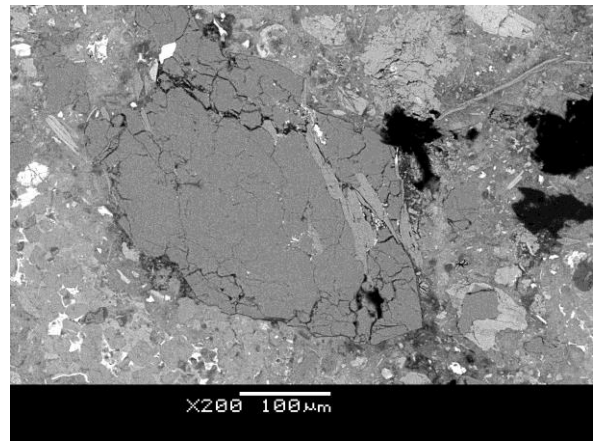
Figure 4-20: Cracks in quartzite aggregate

EURAD (Deliverable n° 2.13) - **Intermediate level radioactive waste packages – Characterization of waste and backfill degradation experiments**
Dissemination level: Public
Date of issue of this report: **18/03/2024**

Page 56
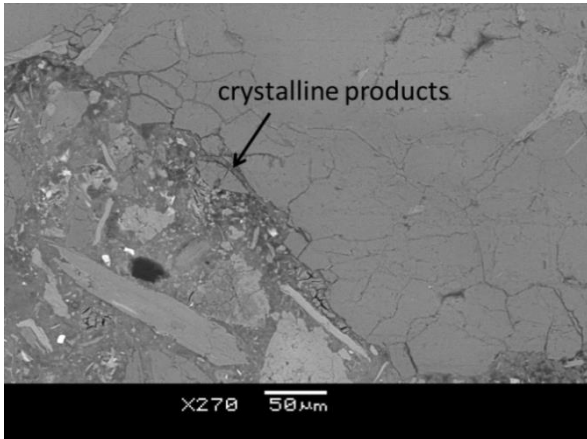
Figure 4-21: Crystalline product (marked by an arrow) within the cracks in quartzite aggregate
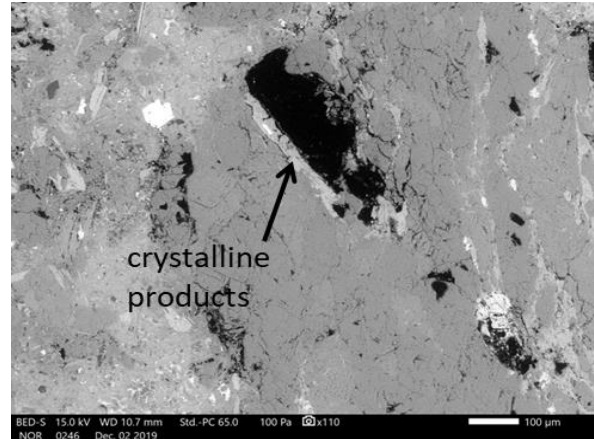
Figure 4-22: Crystalline product (marked by an arrow) inside quartzite aggregate
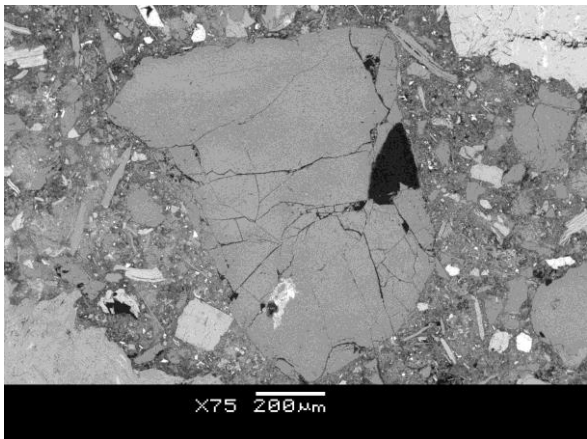
Figure 4-23: Quartz grain is cracked but has sharp, straight edges.
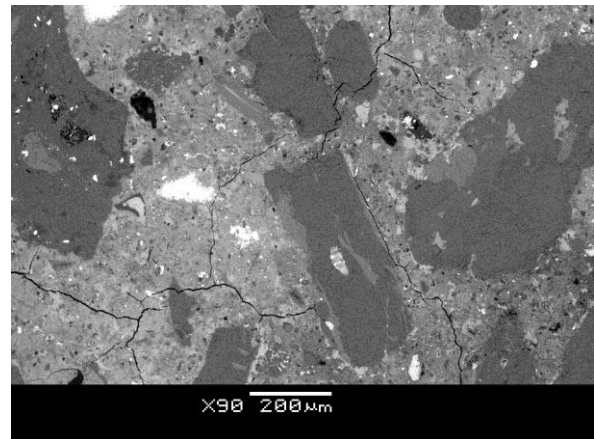
Figure 4-24: Cracks in cement paste and within the quartz grains
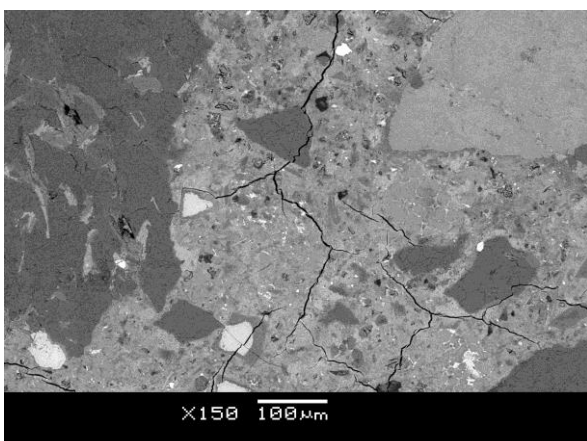
Figure 4-25: Cracks in cement paste and within quartz grains
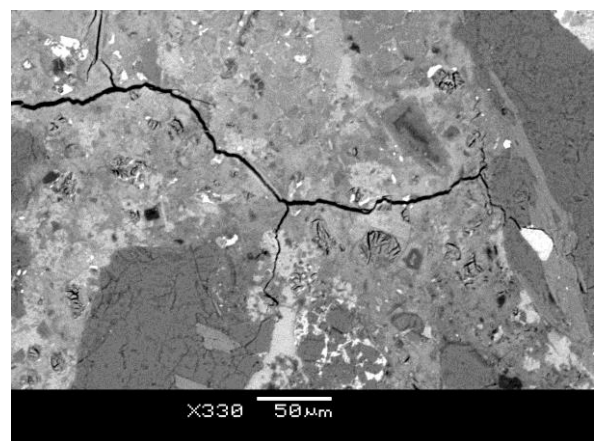
Figure 4-26: Cracks in cement paste and along the grain boundary (in the left hand side)

EURAD (Deliverable n° 2.13) - **Intermediate level radioactive waste packages – Characterization of waste and backfill degradation experiments**
Dissemination level: Public
Date of issue of this report: **18/03/2024**

Page 57
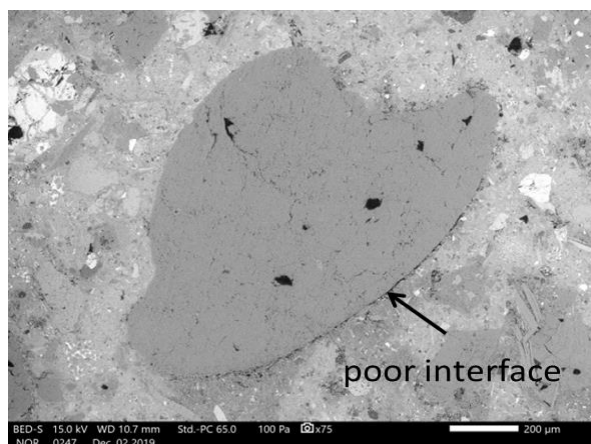
Figure 4-27: Poor contact between quartz grain and matrix
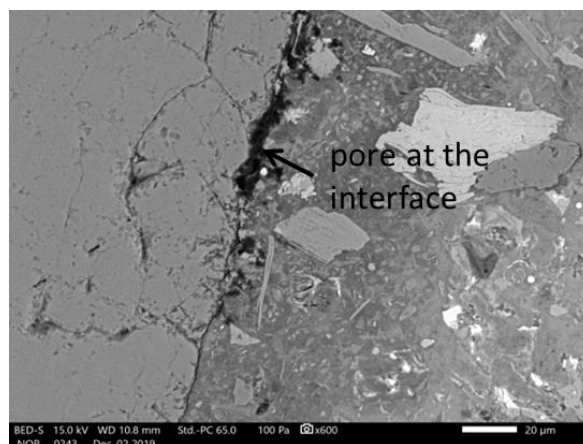
Figure 4-28: Porosity at the interface between quartz grain and matrix

Concrete samples from the Ozbalt hydroelectric power plant

In all four concrete samples (V1 – V4) signs of ASR have been observed. Grains of siliceous aggregate (both coarse and fine) exhibit ASR which is manifested in the form of micro cracks in quartz grains (Fig. 4-29), and micro cracks in quartzite, gneiss in other siliceous grains containing quartz as one of the main constituents. This indicates that the silica cement binding the subgrains in these petrographic types dissolves more readily than the subgrains themselves (Fig 4-30). In contrast to the samples from the Fala hydroelectric power plant, the dissolution of the siliceous grains appears more advanced. Many micro cracks intersecting cement matrix running from aggregates into hardened cement paste have been observed. The reaction products are either a lime-alkali-silica gel, which was identified on the surface of the samples V1 and V2 (Fig. 4-31) or microcrystalline product which was observed in the cement matrix and with morphology of the gel surrounding a flint particle, with the corresponding chemical spectrum in Figure 3-32. The CaO/SiO_2 ratio of the gel was between 0.3 and 1.6. Large amounts of ettringite were also found filling cracks in the cement paste and along the siliceous grains.

All samples were taken at the exposed locations of the Ozbalt hydroelectric power plant. There are no significant differences between examined samples (V1 – V4). The signs of reaction in their features

EURAD (Deliverable n° 2.13) - **Intermediate level radioactive waste packages – Characterization of waste and backfill degradation experiments**
Dissemination level: Public
Date of issue of this report: **18/03/2024**

Page 58
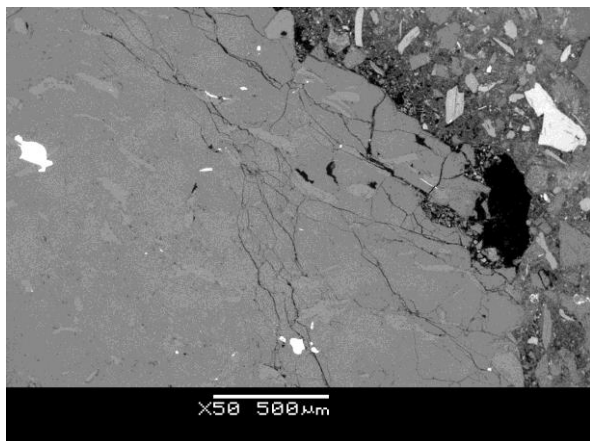
Figure 4-29: Micro cracks in quartz grain
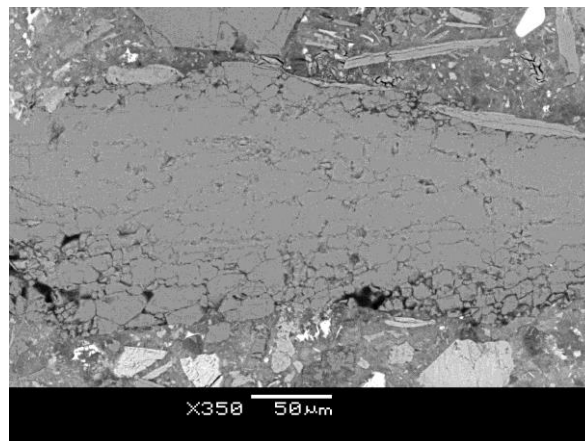
Figure 4-30: Dissolution of cement between quartz grains in sandstone
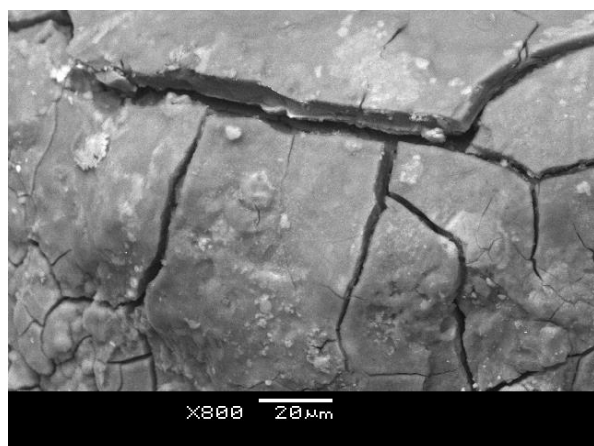
Figure 4-31: Exudation of Ca-rich gel on the surface of the concrete (sample V2)
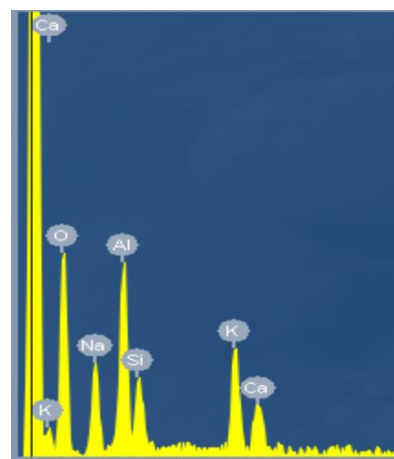
Figure 4-32: Corresponding chemical spectrum of the gel

Concrete samples from the Mariborski otok hydroelectric power plant

Concrete samples from the Mariborski otok hydroelectric power plant exhibit only slight signs of reaction or degradation. Individual grains of quartz with cracks and dissolution features were detected (Figs. 4-33, 3-34 and 4-35). The fine aggregates are affected while the coarse grains do not show any indications of degradation. In some pores precipitation of ettringite has been observed (Fig. 4-36).

Dissolutions areas in quartz also occur (Fig 4-34), in the direction from the outside towards the interior of the grain. Neither reaction products nor cracks across the cement paste were observed.

EURAD (Deliverable n° 2.13) - **Intermediate level radioactive waste packages – Characterization of waste and backfill degradation experiments**
Dissemination level: Public
Date of issue of this report: **18/03/2024**

Page 59
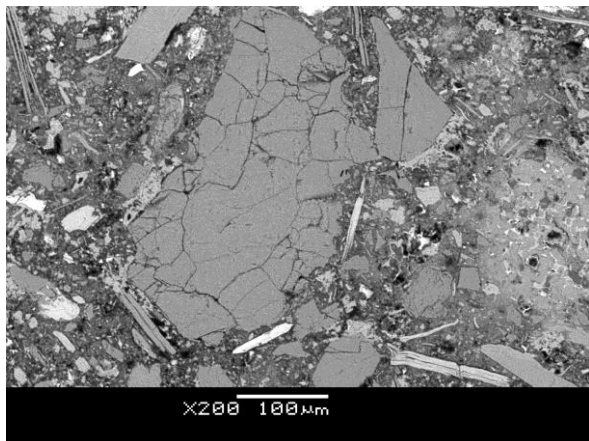
Figure 4-33: Micro cracks in quartz grain (sample M1)
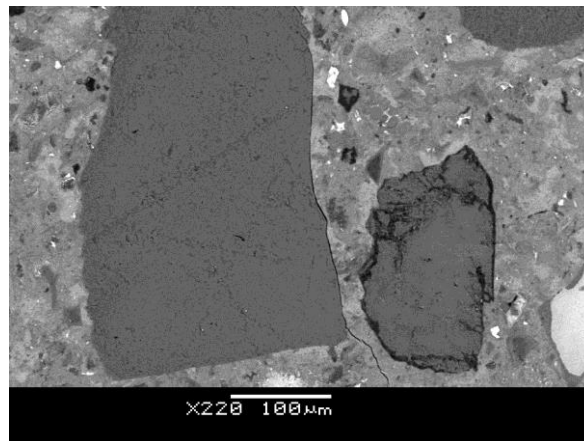
Figure 4-34: Crack along quartz boundary (large grain) and dissolution rim of quartz (small grain) (sample M2)
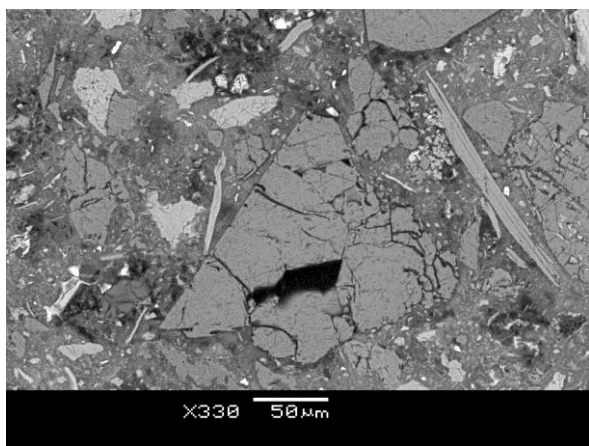
Figure 4-35: Micro cracks in quartz grain (sample M2)
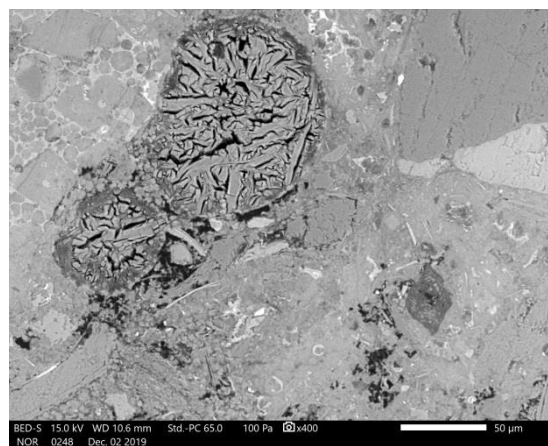
Figure 4-36: Ettringite in air void (sample M2)

4.1.3.1.2   Investigation of old concrete samples with micro-XRD (PSI)

Micro-XRF/XAS investigations have been performed on samples taken from a 105-year-old hydroelectric power plant dams in Fala/Slovenia. The Fala samples were taken from indoor space, but from concrete with high humidity conditions. Concrete sample from core F1 was prepared as thin sections (~30 micrometer thick). The micro-XRF/XAS experiments were conducted at the PHOENIX I beamline of the Swiss Light Source (SLS). The PHOENIX beamline is an undulator based beamline, operating in the energy range from 0.3-8 keV, with options of unfocused (1.5 by 1.5 mm) or focused beam (ca. 2 by 2 µm). Monochromatic light is generated by a double crystal monochromator (Si 111). Powder samples (mountainite, shlykovite, SKC, SNC and K_CSH) were spread on conducting carbon adhesive tapes, and then attached to a copper plate together with the polished sample. The plate was mounted on a sample stage in a vacuumed chamber (~10^{-5} mbar). The X-ray fluorescence signal was recorded using a 4-element energy dispersive silicon drift Vortex detector (SDD). Two-dimensional element mappings were obtained for field sample by scanning the sample through the micro-focused beam (beam size: ~2 µm (vertical) x ~2 µm (horizontal)) with the incident beam energy fixed at 4050 eV (slightly above the Ca K-edge). Mapping of the elemental distribution of Ca, Si, K and S was carried out at selected three regions. When points of interest (POI) were located, the incident beam energy was scanned to obtain the absorption spectra from 3980 to 4200 eV for the Ca K-edge. The

EURAD (Deliverable n° 2.13) - **Intermediate level radioactive waste packages – Characterization of waste and backfill degradation experiments**
Dissemination level: Public
Date of issue of this report: **18/03/2024**

Page 60

XANES spectra were normalized and processed using the Athena package (Ravel and Newville 2005).

Experimental results

The XRF maps of the three regions for Ca, Si, K and S are shown in **Erreur ! Source du renvoi introuvable.**37 to **Erreur ! Source du renvoi introuvable.**9. Crosses indicate where micro-XANES spectra were collected. The micro-XRF maps collected at the Ca edge show a very heterogeneous distribution (**Erreur ! Source du renvoi introuvable.**29 to **Erreur ! Source du renvoi introuvable.**1). Ca and K maps show in all regions a good correlation. In regions with a high S concentration an anti-correlation with Ca, Si and K was observed. The Ca XANES spectra of POI are shown in **Erreur ! Source du renvoi introuvable.**37 to **Erreur ! Source du renvoi introuvable.**. No indication for alteration processes on the micro-scale was detected in the XRF maps, indicating that the humidity was not sufficient to foster concrete damage due to long-term physiochemical processes. The employed spatial resolution of ~2 x ~2 µm in the micro-XRF maps does not allow gaining insights on processes which occur on the nano-scale. Furthermore, no information on lighter elements below the Si-K-edge could be obtained at the PHOENIX I beamline. Therefore, SEM/EDX investigations could provide valuable informations with nano-scale spatial resolution and on light elements such as Mg and Al.

Numbers 1-8 in the map of region 1 indicate point of interests (POI) where micro-XAS spectra were collected (**Erreur ! Source du renvoi introuvable.**29 to **Erreur ! Source du renvoi introuvable.**1). The data can be grouped in three categories: a) consisting of POI 4, 5 and 7, b) consisting of POI 2 and 3, c) consisting 1, 6, and 8. The spectra of the group a) show similarities to the references shlykovite and amourphous CSH phases. For the spectra in group b) no known reference spectra was found to produce a good match. The spectra of group c) seem to be a mixture of groups a) and b). The formation of mountanite and ASR-P1 can be excluded. In the POI of region 2 no spectra (11-23) match the references, ASR-P1, mountanite, shlykovite or CSH. Instead, they show similarities to the unknown phase of POI 2. In the region 3 the POI 26-31 show similarities to shlykovite and amourphous CSH phases. The spectra of POI 24, 25 and 30 are again similar to the unknown phase of e.g. POI 2, 3, 11-23, 24-25, 30.

EURAD (Deliverable n° 2.13) - **Intermediate level radioactive waste packages – Characterization of waste and backfill degradation experiments**
Dissemination level: Public
Date of issue of this report: **18/03/2024**

Page 61
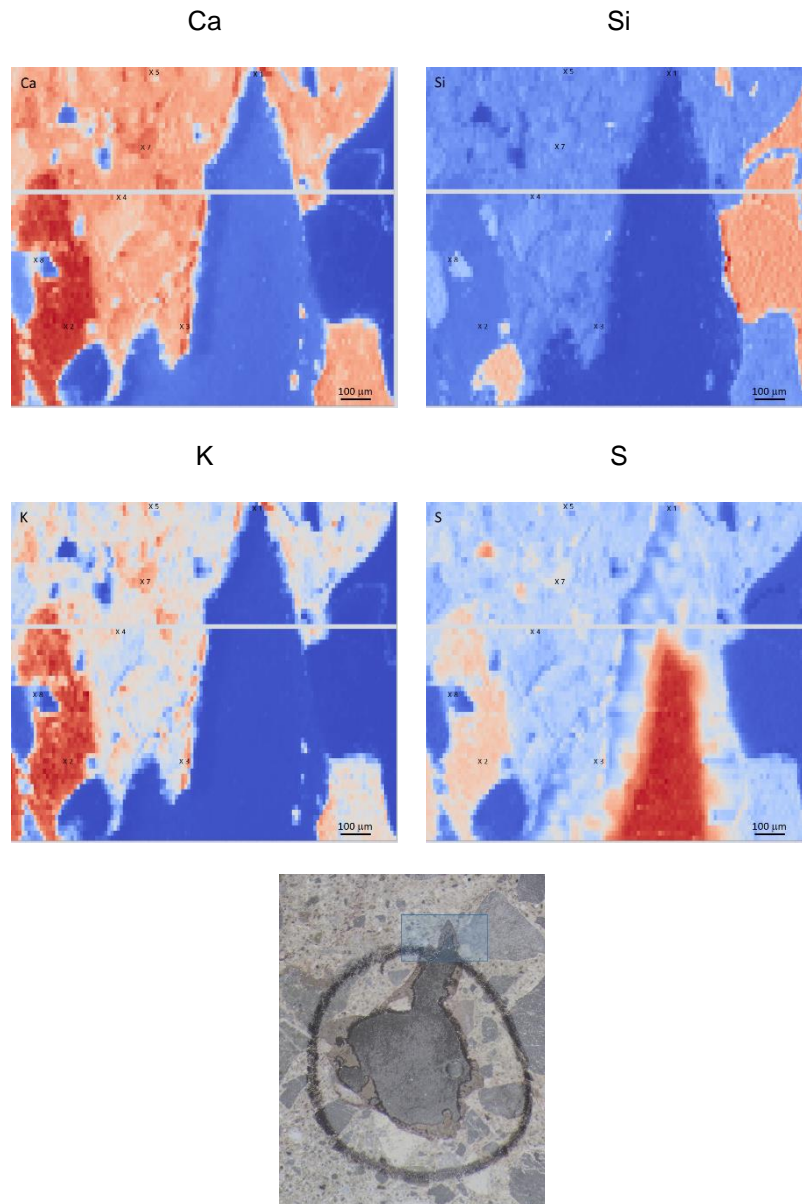
Figure 4-37: XRF maps of region 1 (blue colours indicate low and red high concentrations) and an optical image (the square indicates where the XRF maps have been collected)

EURAD (Deliverable n° 2.13) - **Intermediate level radioactive waste packages – Characterization of waste and backfill degradation experiments**
Dissemination level: Public
Date of issue of this report: **18/03/2024**

Page 62
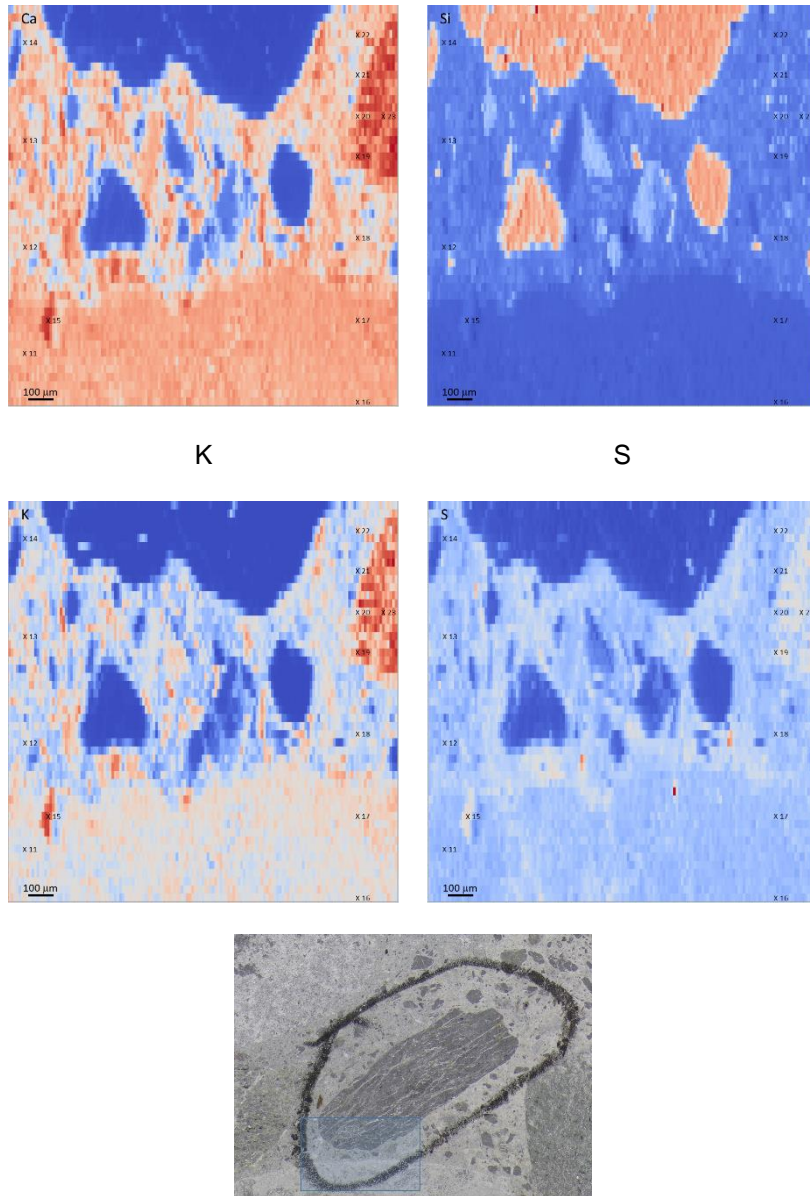
Figure 4-38: XRF maps of region 2 (blue colours indicate low and red high concentrations) and an optical image (the square indicates where the XRF maps have been collected)

EURAD (Deliverable n° 2.13) - **Intermediate level radioactive waste packages – Characterization of waste and backfill degradation experiments**
Dissemination level: Public
Date of issue of this report: **18/03/2024**

Page 63
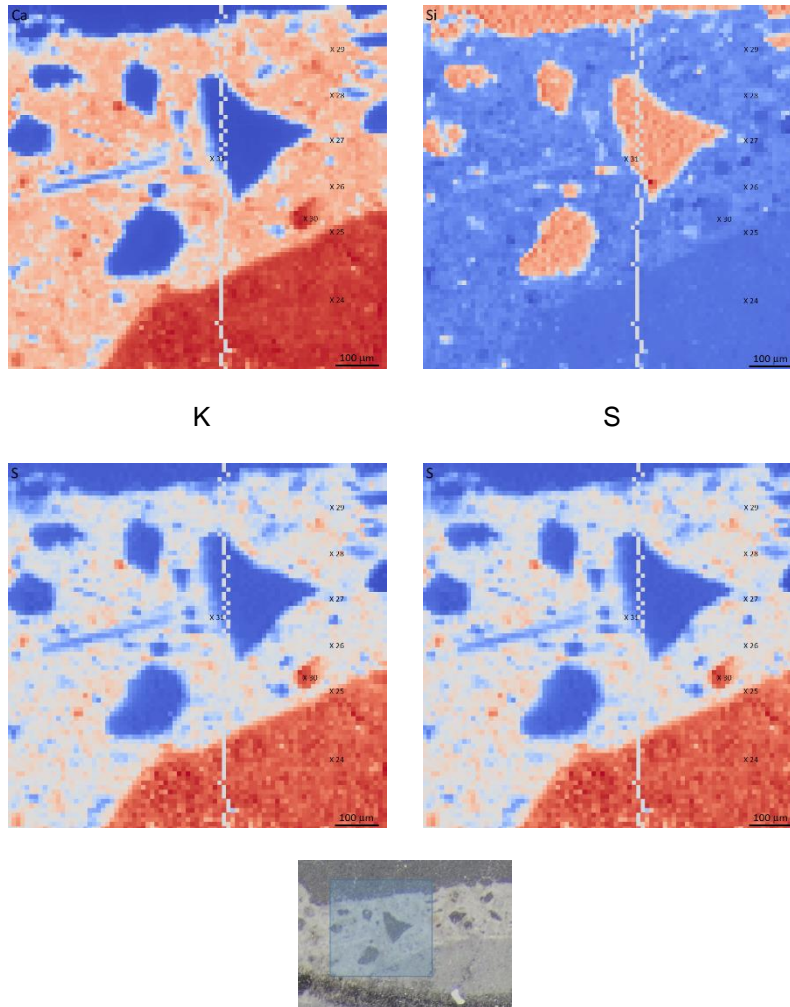
Figure 4-39: XRF maps of region 2 (blue colours indicate low and red high concentrations) and an optical image (the square indicates where the XRF maps have been collected)

EURAD (Deliverable n° 2.13) - **Intermediate level radioactive waste packages – Characterization of waste and backfill degradation experiments**
Dissemination level: Public
Date of issue of this report: **18/03/2024**

Page 64
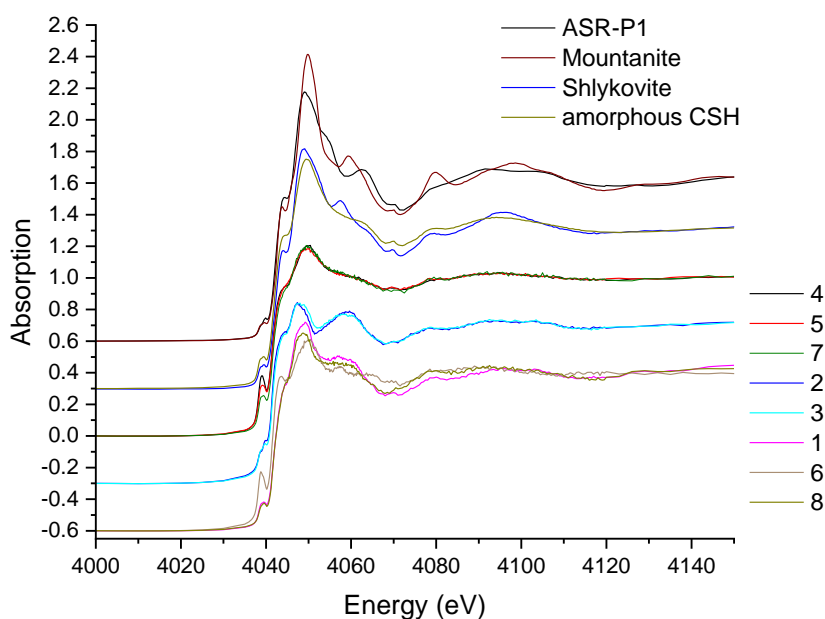
Figure 4-40: Ca micro-XANES spectra (1-8), with selected references collected of region 1
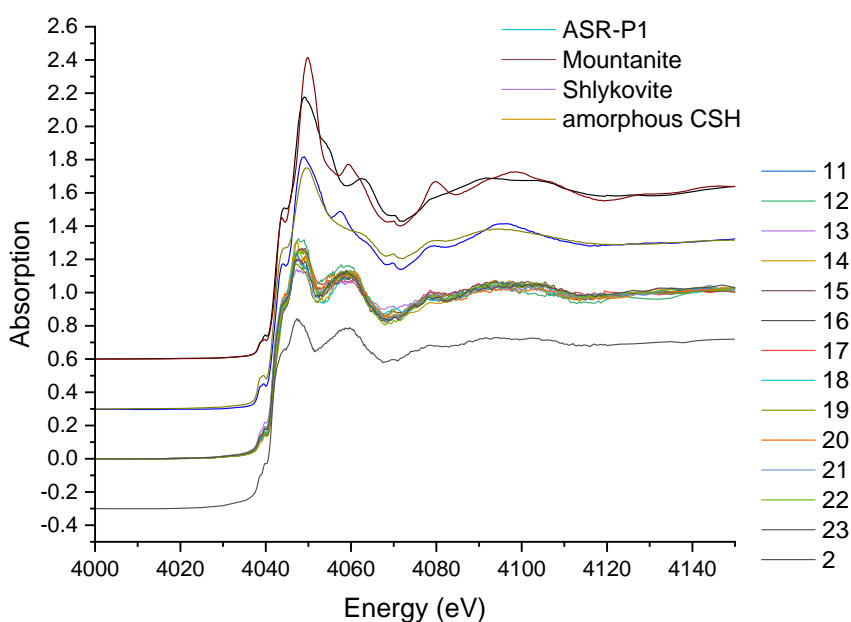
Figure 4-41: Ca micro-XANES spectra (11-23), with selected references collected of region 2. The Ca micro-XANES spectra of POI 2 of region 1 is plotted for comparison

EURAD (Deliverable n° 2.13) - **Intermediate level radioactive waste packages – Characterization of waste and backfill degradation experiments**
Dissemination level: Public
Date of issue of this report: **18/03/2024**

Page 65
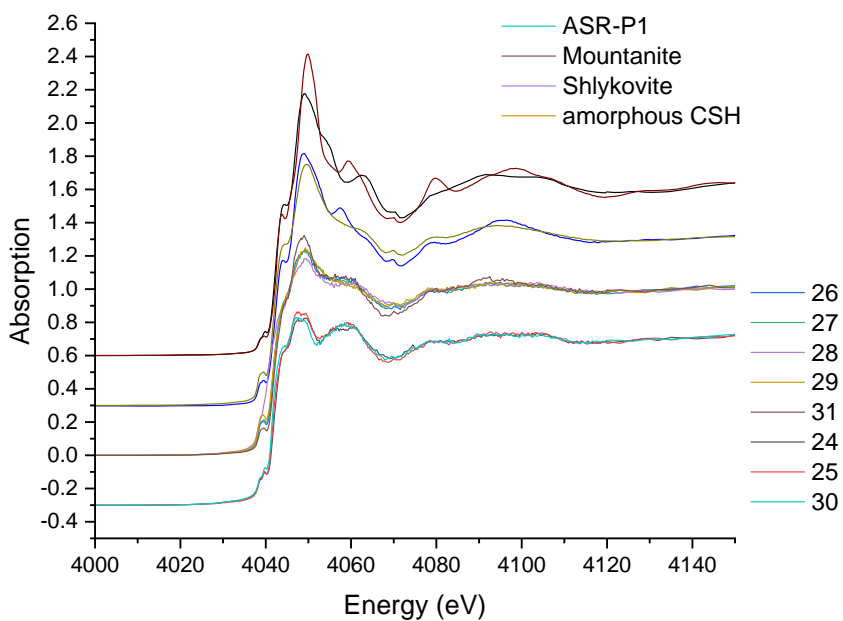
Figure 4-42: Ca micro-XANES spectra (26-30), with selected references collected from region 3

EURAD (Deliverable n° 2.13) - **Intermediate level radioactive waste packages – Characterization of waste and backfill degradation experiments**
Dissemination level: Public
Date of issue of this report: **18/03/2024**

Page 66

5. Conclusion and input towards modelling

The results and the main outcomes for each individual experiment are presented below. In general, the experimental results on cementitious composites shows the high importance of maintaining a high pH value in a repository. The high pH protects the materials against carbonation, because microbial degradation of organic waste is suppressed. Furthermore, metal corrosion is slowed down at high pH. The use of non-reactive, mineralogical stable aggregate is also a prerequisite for manufacturing of high-quality, dense concrete with long durability.

Gas generation experiment (Chapter 2)

The long-term and large-scale in situ Gas Generation Experiment (GGE) established in Olkiluoto, Finland has provided us with extensive and comprehensive data. The data includes the aspects of the rate and composition of generated gas, the aqueous geochemistry, and microbe populations present at various locations within the experiment. A significant observation from the GGE was that the pH conditions were heterogeneous (pH 6 to 11), providing optimal neutral pH niches for microbial activity from the outset of the experiment. Over the extended time scale of the experiment, chemical conditions were stabilized and differences in the microbial abundances and community structure in various GGE compartments became less significant. The results demonstrate that organic matter in LLW is converted to methane and carbon dioxide (CO_2) by a succession of anaerobic processes within a complex microbial consortium. An amount of CO_2 generated from waste reacts with concrete, which induces chemical degradation of concrete, i.e., carbonation. Portlandite is therefore consumed with calcite precipitating. The pH value of the carbonated cement paste first drops to around 10 when all portlandite is consumed and later to a pH of around 8, when the other phases are decomposed. The low pH may induce corrosion of steel bars, which further degrades the performance of reinforced concrete structures. In addition, the leaching of soluble chemical components gradually leads to the depletion of the components that bind the cement. Therefore, the mechanical strength and the stiffness of the concrete will decrease as a result of leaching. Leaching also increases the porosity of the concrete thereby increasing their diffusivity and hydraulic conductivity. Chemical environment evolution inside the waste package is thus changing and it has evident implications on the performance of disposal cells.

The data gathered from GGE is an important input for modelling. The experiment provides data for biogeochemistry modelling of gas production. The modelling work has been completed and the corresponding model is reported in ACED deliverable D2.15. Moreover, the measured gas generation rates are precious input for predicting the durability performance of concrete, e.g., carbonation. The upscaling modelling from the waste package to the disposal cell has been planned in ACED, and the work is reported in ACED deliverable D2.19.

Waste package concrete experiment (Chapter 3)

The predictive capability of models simulating the chemical evolution depend on the accuracy of input parameters such as reaction rate, diffusivity and permeability and their changes as the distribution in size of pores evolve due to chemical interactions. The relative humidity and temperature dependent oxygen and carbonation profiles at 5°C and 20°C for concrete with the same cement content but different porosity allow a determination of an accurate reaction rate.

The porosity has gravimetrically been determined from concrete samples with a representative size after 1000 days exposure to a relative humidity of 6% at 20°C: 13% for waste package concrete and 21% for foamed concrete. The van Genuchten parameters and characteristic pore radius obtained from the water retention curves have been used to determine the water saturated permeabilities for the investigated two types of concrete with the equation determined by Millington and Quirk. As the

EURAD (Deliverable n° 2.13) - **Intermediate level radioactive waste packages – Characterization of waste and backfill degradation experiments**
Dissemination level: Public
Date of issue of this report: **18/03/2024**

Page 67

water saturation is higher at lower relative humidity's for concrete compared to cement paste, it is tentatively proposed that reaction rims between quartz aggregates and cementitious fluid made upon hardening of concrete result into a finer refined pore structure. Consequently, the cementitious phase within hardened concrete is less permeable than solely hardened cement paste.

COVRA's waste package concrete is impermeable in engineering terms but the effect of temperature and relative humidity after exposure to air for 1000 days can clearly be observed in the reaction fronts in which trace amounts of iron-sulphide have reacted while carbonation profiles can hardly be observed. The carbonation profiles have been determined from sprayed freshly broken concrete surfaces in order to prevent reaction with non-hydrated cement particles. Also, a chemical effect by exposure to a solution as saline seawater for $4\frac{1}{3}$ years, could not been deduced from cut samples that had been pulverized.

The investigated foamed concrete has a 1.6 times large porosity than COVRA's waste package concrete. This difference in porosity had a high impact: trace amounts of iron-sulphide have uniformly reacted at almost any relative humidity i.e. clear reaction fronts as observed for waste package concrete are not visible. After exposure to air for 1000 days, carbonation profiles are clearly visible but a relation with the relative humidity could not been observed. Magnesium enrichment could be deduced from analysis of the measurements after exposure to a solution as saline seawater for $4\frac{1}{3}$ years from cut samples that had been pulverized.

Aggregate-cement reactions in concrete (Chapter 4)

Investigation of the presence of aggregate-cement reactions in concrete cores taken from three hydro technical dams on the Drava River, the oldest of which is 120 years old, confirmed aggregate-cement reactions in all samples, regardless of whether they were taken outside or inside. Samples taken outside are more affected; however the damage also depends on the porosity of the samples. The main driver of aggregate-cement reactions is siliceous aggregate (deformed quartz, quartzite, gneiss, sandstone), which is slowly reactive due to its mineralogical characteristics and history. Damage manifests itself as cracks around the aggregate grain and in the aggregate itself, as the dissolution of the grains and as the formation of reaction products, which are both gel and crystalline products. The alkali content of the cements, the types of cements used in structures and water saturation history were unknown, therefore this experiment was not modelled in Subtask 3.3. However, some basic facts to be considered in the concrete design are: (i) knowledge of the aggregate in terms of the petrographic composition and proportions of potentially reactive components, (ii) speed, extent and mechanism of the reaction in an alkaline medium, (iii) potential "pessimum content" of the aggregate and the risk of alkali release from of the aggregate itself, (iv) the composition of the cement, especially with regard to the quantity of water-soluble alkali and mineral/chemical additives, (v) quality of the concrete and (vi) the environmental conditions during its lifetime.

EURAD (Deliverable n° 2.13) - **Intermediate level radioactive waste packages – Characterization of waste and backfill degradation experiments**
Dissemination level: Public
Date of issue of this report: **18/03/2024**

Page 68

6. References

Betonpocket, (2019). Betonpocket 2020, Betonhuis.

Erika Neeft, E. J. (2022). Initial State of the Art on the assessment of the chemical evolution of ILW and HLW disposal cells. EURAD Deliverable 2.1.

Finnish Biocycle and Biogas Association web-page (2022).

Godart, B., de Rooij, M. and Wood, J. G.M., 2013.Guide for Diagnosis and Appraisal of AAR Damage to Concrete Structures, Part 1 Diagnosis (AAR 6.1) RILEM State-of-the-Art Reports, Vol. 12

Höglund, L. (2014). The impact of concrete degradation on the BMA barrier functions. Solna: SKB R-13-40.

I&E, (2016). The national programme for the management of radioactive waste and spent fuel, Ministry of Infrastructure and the Environment (I&E), The Hague, Netherlands, Parliamentary papers, session year 2015-2016, 25422, No. 149.

Jackson, M.D., Mulcahy, S.R., Chen, H., Li, Y., Li, Q., Cappelletti, P., and Wenk, H.-R., (2017). Philipsite and Al-tobermite mineral cements produced through low-temperature water-rock reactions in Roman marine concrete, American Mineralogist, v. 102, no. 7, p. 1435-1450.

Jensen, V. 1993. Alkali Aggregate Reaction in Southern Norway, doctoral thesis, Technical University of Trondheim, NTH, Norway: pp 265 +10 Appendices.

Leivo, M. S.-N. (2011). Effect of interacted deterioration parameters on service life of concrete structures in cold environments. Espoo: VTT-R-09119-11.

Lemmon, E.W., (2015). Vapor pressure and other saturation properties of water, CRC Handbook of Chemistry and Physics, CRC Press Taylor and Francis Group, p. 6-5.

Lothenbach, B., Le Saout, G., Ben Haha, M., Figi, R., and Wieland, E., (2012). Hydration of a low-alkali CEM III/B–SiO2 cement (LAC), Cement and Concrete Research, v. 42, p. 410-423.

Matala, S. (1995). Effect of carbonation on the pore structure of granulated blast furnace slag concrete. Espoo: Helsinki University of Technology.

Mazurek, M., Gautschi, A., Marschall, P., Vigneron, G., Lebon, P., and Delay, J., (2008). Transferability of geoscientific information from various sources (study sites, underground rock laboratories, natural analogues) to support safety cases for radioactive waste repositories in argillaceous formations, Physics and Chemistry of the Earth, v. 33, p. S95-S105.

Merz, C., F. Hunkeler and A. Griesser (2006). Schäden durch Alkali-Aggregat-Reaktion an Betonbauten in der Schweiz. Forschungsauftrag AGB2001/471. UWEK. UWEK, Forschungsauftrag AGB2001/471, Bericht Nr. 599, Bern. Bericht Nr. 599.

Millington, R.J., and Quirk, J.P., (1961). Permeability of porous solids, Transactions of the Faraday society, v. 57, p. 1200-1207.

Mladenovic, A., Neeft, E., Deissmann, G., Dähn, R., Geng, G., Koskowski, G., and Markku, L., (2019). ILW: Report describing the selected experiments and the existing/expected experimental results. Final version as of 24.12.2019 of deliverable D2.11 of the HORIZON 2020 project EURAD. EC Grant agreement no: 847593., ejp-eurad.eu, p. 51.

EURAD (Deliverable n° 2.13) - **Intermediate level radioactive waste packages – Characterization of waste and backfill degradation experiments**
Dissemination level: Public
Date of issue of this report: **18/03/2024**

Page 69

NAGRA, (2008). Effects of post-disposal gas generation in a repository for low- and intermediate-level waste sited in the Opalinus Clay of Northern Switzerland, NAGRA Technical report 08-07, www.nagra.ch.

Neeft, E., de Bruin, T., van Kleef, R., Phung, Q.T., Perko, J., Seetharam, S., Mijnendonckx, K., Li, X., Hausmannová, L., Vašíček, R., Večerník, P., Hlaváčková, V., Černá, K., Černoušek, T., Helson, O., Bourbon, X., Zghondi, J., Vidal, T., Sellier, A., Shao, J., Rougelot, T., Jantschik, K., Kulenkampff, J., Deissmann, G., Griffa, M., Churakov, S., Gimmi, T., and Ma, B., (2021). Selected experiments for assessing the evolution of concrete, their mechanical safety function and performance targets. Final version as of 28.01.2022 of deliverable D16.3 of the HORIZON 2020 project EURAD. EC Grant agreement no: 847593., http://www.ejp-eurad.eu/.

Neeft, E., Jacques, D., and Deissmann, G., (2022). Initial State of the Art on the assessment of the chemical evolution of ILW and HLW disposal cells. D 2.1 of the HORIZON 2020 project EURAD. EC Grant agreement no: 847593., http://www.ejp-eurad.eu/.

Papadakis, V.G., Vayenas, C.G., and Fardis, M.N., (1991). Experimental modeling and experimental investigation of concrete carbonation, ACI Materials Journal v. 88, no. 4, p. 363-373.

Poyet, S., (2016). Describing the influence of temperature on water retention using van Genuchten equation, Cement and Concrete Research, v. 84, p. 41-47.

Ravel, B. and M. Newville (2005). "ATHENA, ARTEMIS, HEPHAESTUS: Data analysis for X-ray absorption spectroscopy using IFEFFIT." Journal of Synchrotron Radiation 12: 537-541.

Roovers, F., (1994). Vervolgonderzoek naar de capability van het betonaanmaakproces, COVRA report nr. 94080.

Schneider, S., Mallants, D., and Jacques, D., (2012). Determining hydraulic properties of concrete and mortar by inverse modelling, Mater. Res. Soc. Symp. Proc., v. 1475.

Small, J., Nykyri M., Helin, M., Hovi, U., Sarlin, T., Itävaara, M. (2008). Experimental and modelling investigation of the biochemistry of gas production from low and intermediate level radioactive waste. Applied. Geochemistry 23, 13383-1418.

Small, J., Nykyri M., Vikman M., Itävaara M., and Heikinheimo L.. . (2017.). "The biogeochemistry of gas generation from low-level nuclear waste: Modelling after 18 years study under in situ conditions." Applied Geochemistry 84: 360-372.

van Genuchten, M.T., (1980). A closed form equation for predicting the hydraulic conductivity of unsaturated soils, Soil. Sci. Soc. Am. J., v. 44, p. 892-989.

Verhoef, E.V., Neeft, E.A.C., Deissmann, G., Filby, A., Wiegers, R.B., and Kers, D.A., (2016). Waste families in OPERA, OPERA-PU-COV023, www.covra.nl.

Vikman, M. M. (2013). KYT-Research report VTT-R-07011-13. Espoo: VTT.

Vikman M. M., Marjamaaa, K., Nykyrib, M., Small, J., Miettinena, H., Heikinheimod, L., Haavistod, T., Itävaaraa, M. (2017). The biochemistry of gas generation from low-level nuclear waste: Modelling after 18 years study under in situ conditions. Applied Geochemistry 84, 360-372.

Vikman, M. M. (2019). The biochemisty of gas generation from low-level nuclear waste: Microbiological characterization during 18 years study under in situ conditions. Applied Geochemistry 105, 55-67.

EURAD (Deliverable n° 2.13) - **Intermediate level radioactive waste packages – Characterization of waste and backfill degradation experiments**
Dissemination level: Public
Date of issue of this report: **18/03/2024**

Page 70

EURAD Deliverable 2.13 – Intermediate level radioactive waste packages – Characterization of waste and backfill degradation experiments

Vikman, M., Sohlberg, E., 2022, The influence of chemical conditions on gas generation in the disposal of low level maintenance waste (KaMu), VTT Technical Research Centre of Finland. 23 p. VTT Research Report; No. VTT-R-00151-22

EURAD (Deliverable n° 2.13) - **Intermediate level radioactive waste packages – Characterization of waste and backfill degradation experiments**
Dissemination level: Public
Date of issue of this report: **18/03/2024**

Page 71